Decentralized Bi-Level Stochastic Optimization Approach for Multi-Agent Multi-Energy Networked Micro-grids with Multi-Energy Storage Technologies

Seyed Ehsan Ahmadi[a], Delnia Sadeghi[a], Mousa Marzband[a,b], Abdullah Abusorrah[b,c], Khaled Sedraoui[b,c]

[a]*Northumbria University, Electrical Power and Control Systems Research Group, Ellison Place NE1 8ST, Newcastle upon Tyne, UK*
[b]*Center of Research Excellence in Renewable Energy and Power Systems, King Abdulaziz University, Jeddah, 21589, Saudi Arabia*
[c]*Department of Electrical and Computer Engineering, Faculty of Engineering, K. A. CARE Energy Research and Innovation Center, King Abdulaziz University, Jeddah 21589, Saudi Arabia*

Abstract

This paper presents a novel decentralized bi-level stochastic optimization approach based on the progressive hedging algorithm for multi-agent systems (MAS) in multi-energy microgrids (MEMGs) to enhance network flexibility. In the proposed model, suppliers and consumers of three energy carrier of power, heat, and hydrogen are considered. This system further consists of multi-energy storage systems such as plug-in electric vehicle aggregators, thermal energy storage, and hydrogen energy storage with the application of power-to-hydrogen and hydrogen-to-power technologies. Furthermore, the Latin Hypercube Sampling method has been utilized to manage the uncertainties. In addition, a penalty function and a power exchange pricing model are evaluated by the electrical marginal price of each microgrid to determine the agreed power exchange among the MEMGs. The suggested work performs over a MAS with three MEMGs. The total profit of each microgrid is maximized over a 24-hour scheduling in three diverse case studies. Ultimately, the proposed decentralized bi-level optimization approach, by converging through seven iterations, indicates an effective performance as a promising solution to a MAS-based framework. Besides, the optimal scheduling of the MEMGs were converged

Email address: mousa.marzband@northumbria.ac.uk Corresponding author (Mousa Marzband)

in the same profit for the diverse network topologies. Implementing multi-energy storage systems plays a major role in increasing total profit of MEMGs and improving the reliability performance of MAS-based structure.

Keywords: Decentralized energy management, multi-energy microgrid, multi-agent system, plug-in electric vehicle, hydrogen energy storage, progressive hedging algorithm.

Nomenclature

Acronyms

BES	Battery Energy Storage
CHP	Combined Heat and Power
DER	Distributed Energy Resource
DS	Distribution system
e-MP	Electrical Marginal Price
EMS	Energy Management System
H2P	Hydrogen to Power
HES	Hydrogen Energy Storage
HFC	Hydrogen Fuel Cell
LHS	Latin Hypercube Sampling
MAS	Multi-Agent System
MEMG	Multi-Energy Microgrid
MT	Micro Turbine
P2H	Power to Hydrogen
PEV	Plug-in Electric Vehicle
PH	Progressive Hedging
PV	Photovoltaic
RO	Robust Optimization

SoC	State of Charge
TES	Thermal Energy Storage
WT	Wind Turbine

Indices

m	Index for MEMGs
i	Index for nodes
g	Index for MTs
c	Index for CHP units and TESs
e	Index for renewable units
v	Index for PEV aggregators
h	Index for HESs
l	Index for tie-lines
t	Index for time
s	Index for scenarios

Parameters

$\underline{P}^{MT}_{(g)}$ / $\overline{P}^{MT}_{(g)}$	Minimum/Maximum allowable active output of MT g (MW)
$\underline{Q}^{MT}_{(g)}$ / $\overline{Q}^{MT}_{(g)}$	Minimum/Maximum allowable reactive output of MT g (MVAR)
$P^{MT,\,RU}_{(g)}$ / $P^{MT,\,RD}_{(g)}$	Active ramp up/down limits of MT g (MW)
$Q^{MT,\,RU}_{(g)}$ / $Q^{MT,\,RD}_{(g)}$	Reactive ramp up/down limits of MT g (MVAR)
$\underline{P}^{CHP}_{(c)}$	Minimum allowable power output of CHP unit c (MW)
$P^{CHP,\,RU}_{(c)}$ / $P^{CHP,\,RD}_{(c)}$	Power ramp up/down limits of CHP unit c (MW)
$UT^{CHP}_{(j)}$ / $DT^{CHP}_{(j)}$	Minimum up/down time of CHP units (hr)
$P^{Load}_{(i,t,s)}$ / $Q^{Load}_{(i,t,s)}$	Active/Reactive load at node i at hour t for scenario s (MW/MVAR)
$H^{Load}_{(i,t,s)}$	Heat load at node i at hour t for scenario s (MWt)
$\underline{B}_{(c)}$ / $\overline{B}_{(c)}$	Minimum/Maximum capacity of TES c (MWht)
$\overline{B}^{ch}_{(c)}$ / $\overline{B}^{dch}_{(c)}$	Maximum charge/discharge rate of the TS c (MWt)
$\underline{E}^{HES}_{(h)}$ / $\overline{E}^{HES}_{(h)}$	Minimum/Maximum capacity of HES h (MW)
$\underline{P}^{P2H}_{(h)}$ / $\overline{P}^{P2H}_{(h)}$	Minimum/Maximum convertible power to hydrogen in HES h (MW)
$\underline{P}^{H2P}_{(h)}$ / $\overline{P}^{H2P}_{(h)}$	Minimum/Maximum convertible hydrogen to power in HES h (MW)

$\overline{P}^{PEV}_{(v)}$	Maximum charge/discharge level of stored power in PEV aggregator v (MW)
$\underline{E}^{PEV}_{(v)}$ / $\overline{E}^{PEV}_{(v)}$	Minimum/Maximum level of stored power in PEV aggregator v (MW)
$E^{PEV,\,RA}_{(v)}$	Allowable ramp of energy storing in PEV aggregator v (MW)
$\overline{P}^{EX}_{(l)}$	Maximum allowable active power exchange for tie-line l (MW)
$\overline{P}^{GR}_{(m)}$	Maximum allowable active power exchange of MEMG m with main grid (MW)
$P^{WT}_{(e,t,s)}$	Power output of WT e at hour t for scenario s (MW)
$P^{PV}_{(e,t,s)}$	Power output of PV e at hour t for scenario s (MW)
$a^{MT}_{(g)}$, $b^{MT}_{(g)}$	Generation cost parameters of MT g
$\phi^{CHP,1}_{(c)}$ - $\phi^{CHP,3}_{(c)}$	Power cost coefficients of CHP unit c
$\psi^{CHP,1}_{(c)}$ - $\psi^{CHP,3}_{(c)}$	Heat cost coefficients of CHP unit c
$PA^{CHP}_{(c)}$ - $PF^{CHP}_{(c)}$	Power operation regions of CHP unit c (MW)
$HA^{CHP}_{(c)}$ - $HF^{CHP}_{(c)}$	Heat operation regions of CHP unit c (MWt)
$r_{(i)}$ / $x_{(i)}$	Line resistance/reactance between node i and i+1 (p.u.)
ϵ	Maximum allowed voltage deviation (%)
λ^{loss} / λ^{gain}	Heat generation loss/excess of CHP units for startup and shutdown interval (%)
η^{TES}	Heat storing efficiency of TESs (%)
$\eta^{PEV,\,ch}$ / $\eta^{PEV,\,dch}$	Charge/Discharge efficiency of PEV aggregators (%)
η^{P2H} / η^{H2P}	Charging/Discharging efficiencies of HESs (%)
$\gamma^{PEV}_{(v)}$	Energy conversion coefficient of PEV aggregator v (MW/km)
$RQ^{PEV}_{(v,t)}$	Distance requirement based on riving pattern of PEV aggregator v at hour t (km)
$SU^{PEV}_{(c)}$ / $SD^{CHP}_{(c)}$	Start-up/Shut-down costs of CHP unit c ($)
$\mu^{EX}_{(l,t)}$	Price of power exchange in tie-line l at hour t ($/MW)
$\mu^{Retail}_{(t)}$	Price of retail electricity market at hour t ($/MW)
$\mu^{Wholesale}_{(t)}$	Price of wholesale electricity market at hour t ($/MW)
$\mu^{Heat,\,Sell}_{(t)}$	Heat price at hour t ($/MWt)
$\mu^{Hyd,\,Sell}_{(t)}$	Hydrogen price at hour t ($/MW)
$\mu^{Hyd,\,Char}_{(t)}$	Charging price of HESs at hour t ($/MW)
$\mu^{PEV}_{(t)}$	Charging and discharging price of PEV aggregators at hour t ($/MW)
$\gamma_{(s)}$	Probability of scenario s [0-1]
M	An adequately large number

Variables

$P^{Flow}_{(i,t,s)}$ / $Q^{Flow}_{(i,t,s)}$	Active/Reactive power flow from node i to node i+1 at hour t for scenario s (MW/MVAR)
$V_{(i,t,s)}$	Voltage magnitude of node i at hour t for scenario s (p.u.)
$\upsilon_{(i,t,s)}$	Additional variable of voltage magnitude of node i at hour t for scenario s (p.u.)
$P^{MT}_{(g,t,s)}$ / $Q^{MT}_{(g,t,s)}$	Active/Reactive power output of MT g at hour t for scenario s (MW/MVAR)
$\pi^{DG}_{(g,t,s)}$ / $\theta^{DG}_{(g,t,s)}$	Additional variable active/reactive power output of MT g at hour t for scenario s (MW/MVAR)
$P^{CHP}_{(c,t,s)}$ / $H^{CHP}_{(c,t,s)}$	Power/Heat generation of CHP unit c at hour t for scenario s (MW/MWt)
$B_{(c,t,s)}$	Available heat in the TES c at hour t for scenario s (MWt)
$SUC^{CHP}_{(c,t,s)}$	Startup cost function of CHP unit c at hour t for scenario s ($)
$SDC^{CHP}_{(c,t,s)}$	Shutdown cost function of CHP unit c at hour t for scenario s ($)
$P^{P2H}_{(h,t,s)}$ / $P^{H2P}_{(c,t,s)}$	Charging/Discharging amount of HES h at hour t for scenario s (MW)
$E^{HES}_{(h,t,s)}$	Level of charge of HES h at hour t for scenario s (MW)
$SOC^{HES}_{(h,t,s)}$	State of charge of HES h at hour t for scenario s (%)
$P^{Hyd,\ Ind}_{(h,t,s)}$	Amount supplied hydrogen to industry in HES h at hour t for scenario s (MW)
$P^{PEV,\ ch}_{(v,t,s)}$ / $P^{PEV,\ dch}_{(v,t,s)}$	Charged/Discharged active power of PEV aggregator v at hour t for scenario s (MW)
$E^{PEV}_{(v,t,s)}$	Stored energy of PEV aggregator v at hour t for scenario s (MW)
$SOC^{PEV}_{(v,t,s)}$	State of charge of PEV aggregator v at hour t for scenario s (%)
$P^{GR,\ Sell}_{(m,t,s)}$	Sell power to main grid in MEMG m at hour t for scenario s (MW)
$P^{GR,\ Buy}_{(m,t,s)}$	Buy power from main grid in MEMG m at hour t for scenario s (MW)
$FG_{(m,t)}(.)$	Function of generating electricity in MEMG m at hour t
$FD_{(m,t)}(.)$	Function of selling electricity in MEMG m at hour t
$P^{EX}_{(l,t,s)}$	Active power exchange of tie-line l at hour t for scenario s (MW)
$P^{EX,\ UP}_{(l,t,s)}$	Active power exchange of tie-line l from MEMG m to neighboring MEMGs at hour t for scenario s (MW)
$P^{EX,\ DO}_{(l,t,s)}$	Active power exchange of tie-line l from neighboring MEMGs to MEMG m at hour t for scenario s (MW)

$X^{UP}_{(l,t,s,\alpha,\beta)}$	Additional variable of active power exchange in tie-line l from MEMG m to neighboring MEMGs at hour t for scenario s (MW)
$X^{DO}_{(l,t,s,\alpha,\beta)}$	Additional variable of active power exchange in tie-line l from neighboring MEMGs to MEMG m at hour t for scenario s (MW)
$\lambda_{(t,\beta)}$	Penalty price of power exchanges at hour t ($/MW)
$\Delta^{EX}_{(l,t,s)}$	Penalty function of tie-line l at hour t for scenario s
$\mathscr{R}^{Load}_{(m,t,s)}$	Revenue function of selling electricity in MEMG m ($)
$\mathscr{R}^{CHP}_{(m,t,s)}$	Revenue function of selling heat in MEMG m ($)
$\mathscr{R}^{PEV}_{(m,t,s)}$	Revenue function of driving requirements in MEMG m ($)
$\mathscr{R}^{HES}_{(m,t,s)}$	Revenue function of supplying hydrogen to industry in MEMG m ($)
$\mathscr{C}^{MT}_{(m,t,s)}$	Cost function of MTs in MEMG m ($)
$\mathscr{C}^{CHP}_{(m,t,s)}$	Cost function of CHP units in MEMG m ($)
$\mathscr{C}^{PEV}_{(m,t,s)}$	Cost function of charging PEVs in MEMG m ($)
$\mathscr{C}^{HES}_{(m,t,s)}$	Cost function of charging HESs in MEMG m ($)
$\mathscr{R}^{GR}_{(m,t,s)}$	Revenue function of selling electricity to main grid in MEMG m ($)
$\mathscr{C}^{GR}_{(m,t,s)}$	Cost function of buying electricity from main grid in MEMG m ($)
$\mathscr{C}^{EX}_{(m,t,s)}$	Cost function of active power exchanges in MEMG m ($)
$\sigma^{MT,\,UC}_{(g,t,s)}$	Commitment state of MT g at hour t for scenario s [0,1]
$\sigma^{SU}_{(g,t,s)}$ / $\sigma^{SD}_{(g,t,s)}$	Start-up/Shut-down state of MT g at hour t for scenario s [0,1]
$\sigma^{CHP,\,UC}_{(g,t,s)}$	Commitment state of CHP unit c at hour t for scenario s [0,1]
$\sigma^{CHP,\,SU}_{(c,t,s)}$ / $\sigma^{CHP,\,SD}_{(c,t,s)}$	Start-up/Shut-down state of CHP unit c at hour t for scenario s [0,1]
$\sigma^{P2H}_{(h,t,s)}$ / $\sigma^{H2P}_{(h,t,s)}$	Charge/ Discharge state of HES h at hour t for scenario s [0,1]
$\sigma^{PEV,\,ch}_{(v,t,s)}$ / $\sigma^{PEV,\,dch}_{(v,t,s)}$	Charge/Discharge state of PEV aggregator v at hour t for scenario s [0,1]
$\sigma^{EX,\,UP}_{(l,t,s)}$	State of power exchange in tie-line l from MEMG m to neighboring MEMGs at hour t for scenario s [0,1]
$\sigma^{EX,\,DO}_{(l,t,s)}$	State of power exchange in tie-line l from neighboring MEMGs to MEMG m at hour t for scenario s [0,1]
$\kappa^{EX}_{(l,t,s)}$	Status of the switch in tie-line l at hour t for scenario s [0,1]

1. Introduction

1.1. Motivations

In recent years, due to issues such as paucity of conventional energy resources, global concerns over climate change, and energy crisis associated with global economic development and manufacturing production, the power system has faced diverse challenges [1, 2]. Generating power and supplying diverse loads via locally available renewable energies have led to the introduction of a novel concept named microgrid [3]. The introduction of novel distributed energy resources (DERs) with diverse renewable energy generation and storage systems in the microgrids have influence remarkable alterations to the conventional energy systems [4]. Furthermore, the microgrids are connected to an adjacent distribution power system, i.e. main grid, to optimize the energy management system by locally distributed resources, and effectively cooperate with the main grid [5, 6]. Higher power network operational flexibility could be also achieved by system operation advancements applying flexible resources and improving grid infrastructure provided by microgrids [7]. On the other hand, the networked structure of the microgrids provides a reliable, highly adaptable and flexible solution to operational objectives of the distribution power system, since each MG contains larger capacity for the consumers through actively managed power exchanges [8, 9].

The numerous energy technologies such as wind turbine (WT), photovoltaic (PV), micro turbine (MT), combined heat and power (CHP), plug-in electric vehicle (PEV), battery energy storage (BES), thermal energy storage (TES), and hydrogen energy storage (HES) have enhanced the microgrid concept to develop an infrastructure called multi-energy microgrid (MEMG), which facilitates multi-energy demands such as power, heating, and hydrogen simultaneously [10]. A MEMG has several terminal resources and several distributed elements for energy generation, conversion, and storage. By applying this network structure, an interconnected energy system with optimized multi-energy resources can be designed. This MEMG is a cost-effective, efficient, and reliable energy system, which could participate in the day-ahead energy markets of electricity, heating, and hydrogen energy carriers

during clearing process of market prices [11]. The CHP units are distributed energy resources (DERs) which can interact with both electrical and thermal energy, as well as energy storages such as BES, TES, and HES in the MEMG to achieve cost-effective results during the scheduling procedure [12, 13]. Furthermore, hydrogen energy is an emerging strategy with zero-emission of carbon [14], which facilitates power-to-hydrogen (P2H) and hydrogen-to-power (H2P) technologies. Also, the HES, a novel storage technology, could apply to P2H/H2P technologies for enhancing economic and ecological features [15].

The multi-agent system (MAS) containing two or more cooperative agents, deploys in MEMGs, which consists of independent agents such as DERs and energy customers. The prime advantages of the MAS-based framework compared to the conventional energy management are self-sufficiency, lower requirement for massive data usage, enhanced robustness, and reliability [16]. The major approaches to perform proper MAS-based energy management in MEMGs are classified into two main groups including centralized and decentralized control frameworks. The centralized system accompanied with a central controller agent to collects overall data from the energy resources, system parameters, cost functions, and technical constraints. The prime benefits of the centralized control framework are reliability and controllability in contrast to disadvantages including multiple communication and computation burdens which could be occurred by single-point failure. On the other hand, the decentralized framework is more robust and less intricate, where the agents based on the applied structure, which is hierarchical or distributed strategies. In this system, the limited data is permitted to exchange between the local controllers [17]. Hence, decentralized energy management is capable to operate the networked MEMGs in a MAS structure with diverse network topologies. Besides, diverse sub-systems in a MAS-based MEMG are associated with diverse stakeholders. Therefore, data sharing without privacy protection may result in critical economic losses. Although market competition enhances the productive participation, it is complex to develop a centralized controller for the MAS to regulate these agents due to the market privacy. Thus, how to realize an efficient operation for MAS-based MEMGs with minimal data exchange becomes an essential challenge [18].

Accordingly, in order to properly characterize optimal scheduling of MAS-based system with networked MEMGs, subject to the uncertainties and network energy balance constraints, in this paper, a novel decentralized bi-level stochastic optimization algorithm is proposed.

1.2. Literature Review

Numerous studies have been previously observed with respect to optimization approaches of MAS in networked MEMG. The authors in [19] propose a stochastic price-based planning strategy for a MEMG. This strategy considers the energy carriers' prices as the uncertain parameters. The outcomes show 6.6% and 50.9% cost saving for winter and summer days, respectively, when the power is offered to the distribution system. A resilience-oriented scheduling structure has investigated in the study [20], for industrial parks, powered with integrated electricity-heat-hydrogen microgrids, which focuses on the demand survivability improvement under contingency conditions. Further, the presented resilient operation problem is reformulated as a CVaR-based stochastic problem, while a risk-averse (RA) method has established to manage the uncertainty of system contingencies. The results demonstrate that the CVaR measure is significantly reduced by 35.2%, which implies that the lowered possibility of energy load interruption. In [21], an optimal planning scheme has presented to developing multi-carrier networked microgrids, considering load profiles in the various seasons. Diverse multi-energy carriers have applied to form energy hubs that interchange energy with each other and the main electricity/gas networks. The results show when hubs integrate the total daily cost of each microgrid has been improved about 200$. A combined cooling, heating, and power (CCHP) microgrid network has discussed in literature [22], which combines the power-to-gas (P2G) technology with the traditional CCHP microgrid. The results show that P2G device can improve the electricity-gas coupling in the CCHP-P2G system enhancing the stability and economy of the system operation. The authors in [23] have focused on combined cooling, heating, and power microgrid, with multi-carrier energy storage consists of HES, TES, and ice storage under the uncertainties of wind speed and electricity price managed by a hybrid robust-stochastic

framework. Obtained results shows that utilizing HES and multi-energy demand response can reduce the operation cost up to 5% for the studied test system. In [24], a multi-energy retailer is introduced to simultaneously meet both flexible and non-flexible electrical, gas, and heat demands of multi-energy consumers. The results show that utilizing the conversion facilities plays a vital role in increasing the profit of multi-energy retailer up to 32% compared to the traditional retailers. In [25], a bi-level optimization problem is presented to schedule a multi-energy system in the day-ahead wholesale market. The results illustrate the efficacy of the proposed model in manipulating market clearing price in favor of the multi-energy system. In Refs. [19–25], the centralized management approach has been applied for the scheduling of the microgrids with multi-energy carriers. However, the networked structure and the MAS-based frameworks were ignored in the systems.

In [26], a novel bi-level EMS has presented for the optimal scheduling of the networked microgrids under the uncertainties of renewable energies and power loads. The outer-level is regulated the required power exchange and data among microgrids, while the inner-level optimally schedules each on-fault microgrid in an emergency condition. The results demonstrated that the total operational cost of the microgrids in the case with demand response is 1395.234$ less than the case without demand response. The authors in [27] have presented a coordinated energy management system considering the cooperation of hubs in day-ahead markets under the uncertainties of diverse loads, day-ahead market energy price, renewable generation, and EVs parameters. The presented model links the natural gas and district heating grids with the electrical grid. The results show the ability of the proposed strategy to improve the flexibility, security, reliability, stability and operational situation of hubs. In Refs. [26] and [27], a centralized energy management has utilized for the scheduling of the multi-energy carriers. However, the investigation of the MAS-based structure is neglected in these studies. The energy hub concept has been studied in [28] in the case of microgrids to beneficial from the efficiency of microgrids as multi-energy hubs using a decentralized algorithm based on the alternating direction method of multipliers (ADMM) to adjust the optimal operation of the microgrids and exchanged power among microgrids and DS. The

results show that when the robustness level is getting twice, the operation cost of DS increases by 19%. A novel decentralized-distributed adaptive robust optimization (ARO) strategy has demonstrated in [29] to model the efficient distributed operation of multi- microgrids with the uncertainties. The analyses showed that the solution time for each iteration of the ARO strategy is reduced by 47%, which greatly improved the solution efficiency. Zhou et al. [30] have recommended two types of robust decentralized economic dispatch strategies for the coordinated scheduling of microgrids in a DS. The economic dispatch strategy has applied on a modified IEEE 33-bus test DS with three microgrids, while the RO-based decentralized framework was suggested for the uncertainties of renewable energies and loads. The results show that the robustness is enhanced at the expense of adding up to 7.6% of costs. In Refs. [28–30], the MAS-based strategy and application of the PEV and HES were not considered in the test systems.

In the study [31], a reliability evaluation strategy is demonstrated for the MAS with WTs, PEVs, and gas storages in a communication framework. A re-dispatching problem with voltage and gas pressure constraints has also suggested to lessen the scheduling cost. The results demonstrated that the maximum error between distributed and centralized reliability evaluation approach is less than 0.8%, which is caused by random errors due to Monte Carlo simulation. A MAS-based decentralized energy management system (EMS) for a grid-connected microgrid has been proposed in [32]. DERs and loads are modeled as independent agents by a reinforcement learning algorithm to optimize the performance of microgrid and each agent. The results show that the operation costs of microgrid is reduced about 48% in the scenario with learning algorithm compared to the scenario without learning algorithm. However, a single microgrid has considered in the proposed system and the concept of the networked framework has not been studied. The authors in [33] has presented a two-level hierarchical multi-agent EMS for the multi-microgrid systems to maximize the utilization of renewable units over a three-microgrid system. The results indicate that using the proposed strategy, the renewable energy utilization of the entire system is improved by 12.32%. In Ref. [34], an optimal voltage regulation approach has been investigated with the participants of multi-microgrids

based on multiple agent systems. A bi-level game model is also addressed for the voltage control process on a modified IEEE 33-bus system. Based on the simulation results of the proposed bi-level game model, the DNO and microgrids improve the voltage profiles through an iteration bidding process. In Ref. [35], a two-layer multi-agent distributed control strategy with fault tolerance control for MMG systems is presented. The simulated results show that the frequencies and voltages in microgrids stay at the allowed values. In [36], a phased algorithm based on symbiotic organisms search and an advanced MAS-based consensus algorithm is proposed to improve the utilization rate of renewable energies in islanded multi-microgrids. Simulation results demonstrate that the utilization rate of renewable energies can reach 99.99% when the difference between renewable energies and demand is large at some moments. However, a deterministic approach has been applied to energy management and the uncertainty analysis has been neglected. In Ref. [37], a distributed-based energy management framework is proposed using primal-dual method of multipliers in smart network with five different agents including an energy hub, a networked multi-microgrid with three agents and a transportation system. The compared distributed approach with the centralized approach showed a very slight error, which indicates that the approaches have almost equal solutions. Although, the MAS-based structure has considered for the multi- microgrids in [33–37], the MEMG is not taken into account.

1.3. Contributions

Based on the mentioned literature of the MEMG scheduling, it is obvious that:

1. Previous works were failed to propose a decentralized energy management for the optimal operation of the MAS-based networked MEMGs considering the PEV and hydrogen-based energy scheduling;
2. The bi-level stochastic optimization approach has not been investigated for the decentralized control framework of the MAS-based MEMGs;
3. Previous studies have not taken into account P2H and H2P facilities along with HES system as an independent agent in the MAS-based framework;
4. A proper penalty function model has not presented in the literature for the

convergence of the agreed energy exchanges among the MAS-based networked MEMGs in a decentralized framework considering the self-sufficiency of each agent.

To fill this gap out, the proposed model has considered all the mentioned factors with the stochastic behavior of the renewable units, energy demands, and energy carrier prices. The MEMG contains an electricity DS, a heating DS, and a hydrogen energy network, which has coupled by MAS-based network. According to the coupling elements, diverse forms of energy in the MEMG can be generated, converted and stored by the connected sources and storage systems. Accordingly, the CHP units and TESs are applied to manage the heat consumption of local customers. Further, the PEV aggregators investigate the optimization constraints of the transportation agents, and the HES are presented for the hydrogen-based consumers and industry by P2H and H2P technologies.

Table 1 demonstrates a comprehensive comparison between the proposed approach and the literature reviewed. Therefore, this paper proposes a novel flexible decentralized bi-level stochastic optimization approach based on the progressive hedging algorithm for the MAS-based networked MEMGs (including power, heat, and hydrogen carrier) under the uncertainties of the renewable units, power and heat demands, as well as distance requirement of PEVs. Specifically, the Latin Hypercube Sampling (LHS) method has been applied to control the mentioned uncertainties. In addition, a reliable penalty function and a power exchange pricing model are modified based on the electrical marginal price (e-MP) to adjust the energy exchange among the networked MEMGs.

The rest of the paper is laid out as follows. In Section 2, MAS-based networked MEMGs configurations are presented. First, the hydrogen production from renewable generations is reviewed, and then the energy management structure of MAS-based MEMGs and the proposed decentralized bi-level stochastic optimization approach are described. In Section 3, the mathematical modeling of the networked MEMGs is demonstrated. Corresponding results are presented in Section 4 for three diverse scheduling case studies. Finally, the paper is concluded in Section 5.

Table 1: Comparison among different research works on the management strategies of MEMGs

Refs	Networked Structure	Multi-Agent	Energy Carriers	Uncertainty Modeling	Management Strategy		Decentralized Algorithm	Problem Constraints					
					Centralized	Decentralized		HES	CHP	TES	PEV	e-Power Ex. Price	Penalty Function
[19]	✖	✖	Power, Gas, Heat, and Hydrogen	Stochastic	✓	✖	✖	✓	✓	✓	✓	✖	✖
[20]	✖	✖	Power, Heat, and Hydrogen	RA Stochastic	✓	✖	✖	✓	✖	✓	✖	✖	✖
[21]	✖	✖	Power, Heat, and Hydrogen	Deterministic	✓	✖	✖	✓	✓	✖	✖	✖	✓
[22]	✖	✖	Power, Gas, and Heat	Two-Stage RO	✓	✖	✖	✖	✓	✖	✖	✖	✓
[23]	✖	✖	Power, Gas, Heat, Cool, and Hydrogen	RO	✓	✖	✖	✓	✓	✓	✖	✖	✖
[24]	✖	✖	Power, Gas, and Heat	Stochastic	✓	✖	✖	✖	✓	✓	✖	✖	✖
[25]	✖	✖	Power, Gas, Heat, and Hydrogen	Stochastic	✓	✖	✖	✓	✓	✓	✖	✖	✖
[26]	✓	✖	Power	SBA	✓	✖	✖	✖	✖	✖	✖	✓	✖
[27]	✓	✖	Power, Gas, and Heat	Stochastic	✓	✖	✖	✖	✓	✖	✓	✖	✖
[28]	✓	✖	Power and Heat	RO	✖	✓	ADMM	✖	✓	✓	✖	✖	✓
[38]	✓	✖	Power	Two-Stage RO	✖	✓	ADMM	✖	✖	✖	✖	✖	✓
[39]	✓	✖	Power	Two-Stage RO	✖	✓	ATC Algorithm	✖	✖	✖	✖	✖	✓
[29]	✓	✖	Power	RO	✖	✓	Bi-Layer PD-ARO	✖	✖	✖	✖	✖	✓
[30]	✓	✖	Power	Two-Stage RO	✖	✓	ADMM	✖	✖	✖	✖	✖	✓
[31]	✖	✓	Power, Gas, and Heat	Deterministic	✓	✖	✖	✖	✓	✖	✓	✖	✖
[32]	✖	✓	Power and Heat	Random Sampling	✖	✓	RL Algorithm	✖	✓	✖	✖	✖	✓
[33]	✓	✓	Power	Deterministic	✓	✖	✖	✖	✖	✖	✖	✖	✖
[34]	✓	✓	Power	Deterministic	✖	✓	Bi-Level Game Scheme	✖	✖	✖	✖	✖	✖
[35]	✓	✓	Power	Deterministic	✓	✖	✖	✖	✖	✖	✖	✖	✖
[36]	✓	✓	Power	Deterministic	✓	✖	✖	✖	✖	✖	✖	✖	✖
[37]	✓	✓	Power, Gas, Heat, and Water	Stochastic	✓	✖	✖	✖	✓	✖	✖	✖	✖
Proposed Model	✓	✓	Power, Heat, and Hydrogen	LHS	✖	✓	Bi-Level Modified Stochastic PH-based Algorithm	✓	✓	✓	✓	✓	✓

2. MAS-based Networked MEMGs Configurations

2.1. Energy Management Structure of MAS-based MEMGs

This section describes a novel structure of the networked MEMGs and the proposed decentralized MAS-based energy management model. As shown in Figure 1, the MAS-based MEMGs composed of electrical/thermal generators such as CHP unit, MT, renewable units such as PV and WT, energy storage systems such as BES, TES, and HES, HFC as H2P technology, PEV aggregators, as well as electrical, thermal, and hydrogen customers considering multi-energy market based on the energy hub interconnection concept. Besides, the P2H technology containing an AC/DC converter, an electrolyzer, and a compressor is applied as the essential elements to convert electricity into hydrogen in each MEMG. The proposed networked model provides multi-energy exchanging among MEMGs and DS. The relation of the electricity, heat, transportation, and hydrogen operators with multi-energy markets is also demonstrated in Figure 1.

Each MEMG has a decentralized controller to manage its local interactions between diverse energy generations and consumptions. In this paper, each local energy supplier and consumer controls are managed by the local decentralized controller presented in each MEMGs. Accordingly, the local electricity operator as the main operator is responsible for ensuring energy balance between local energy suppliers and consumers, while the heat, transportation, and hydrogen operators can monitor their corresponding energy generators and demands, and determine energy prices for their interactions with the local electricity operator in each MEMG. As the only electrical energy is exchanged among MEMGs, a central EMS is also defined as an independent entity to converge the power exchanges in the decentralized framework.

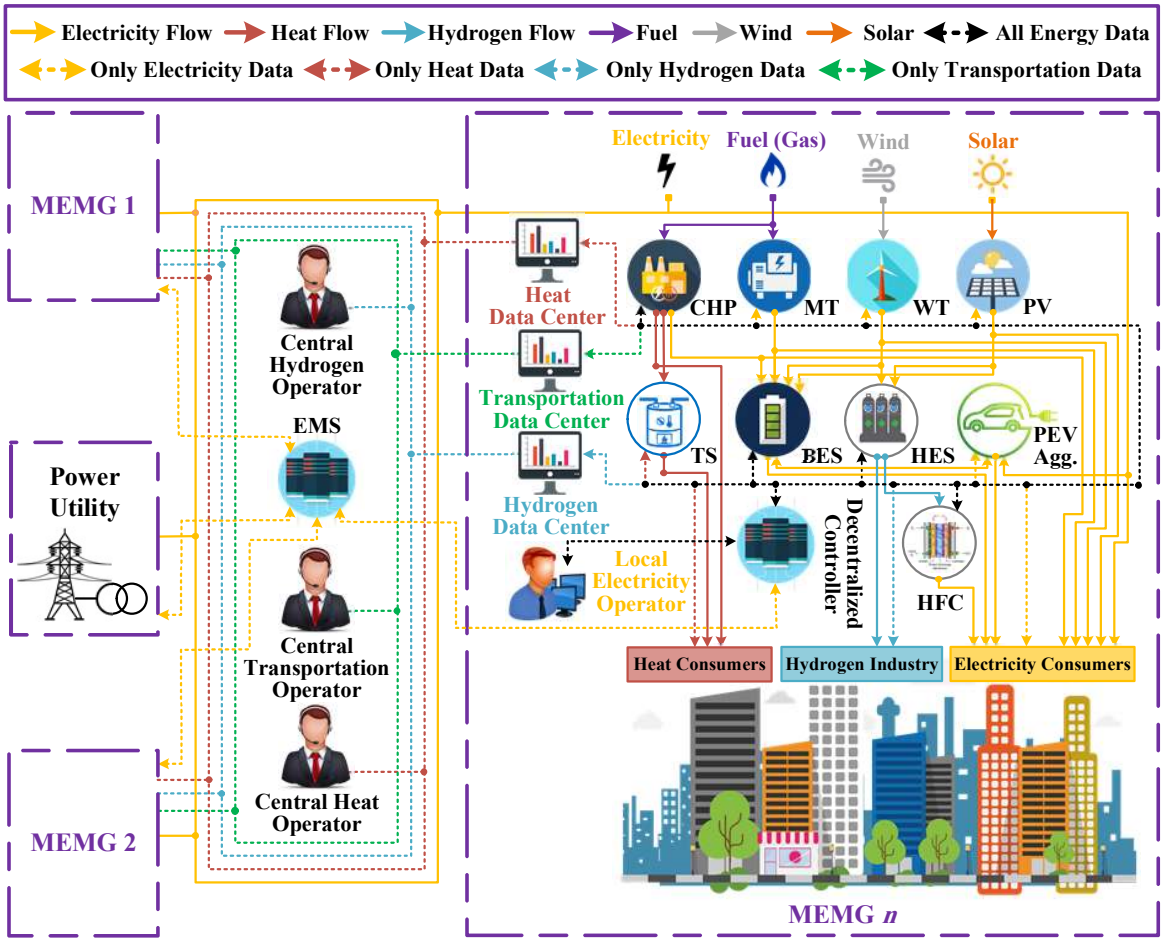

Figure 1: Structure of the networked MEMGs

Figure 2 indicates the proposed MAS-based structure, communication systems, and agent management ontologies of the networked MEMGs to optimally control the energy generation and consumption. As demonstrated in this figure, the operators oversee exchanging required data and energy among MEMGs and the multi-energy market. Given the local energy demands, local energy resources, and energy prices, each MEMG determines its optimal energy management in its decentralized controller. Applying this model leads to the privacy protection for each MEMG and reduces the total computational time for energy management of the networked MEMGs. The definition of different components in Figure 1 as follows:

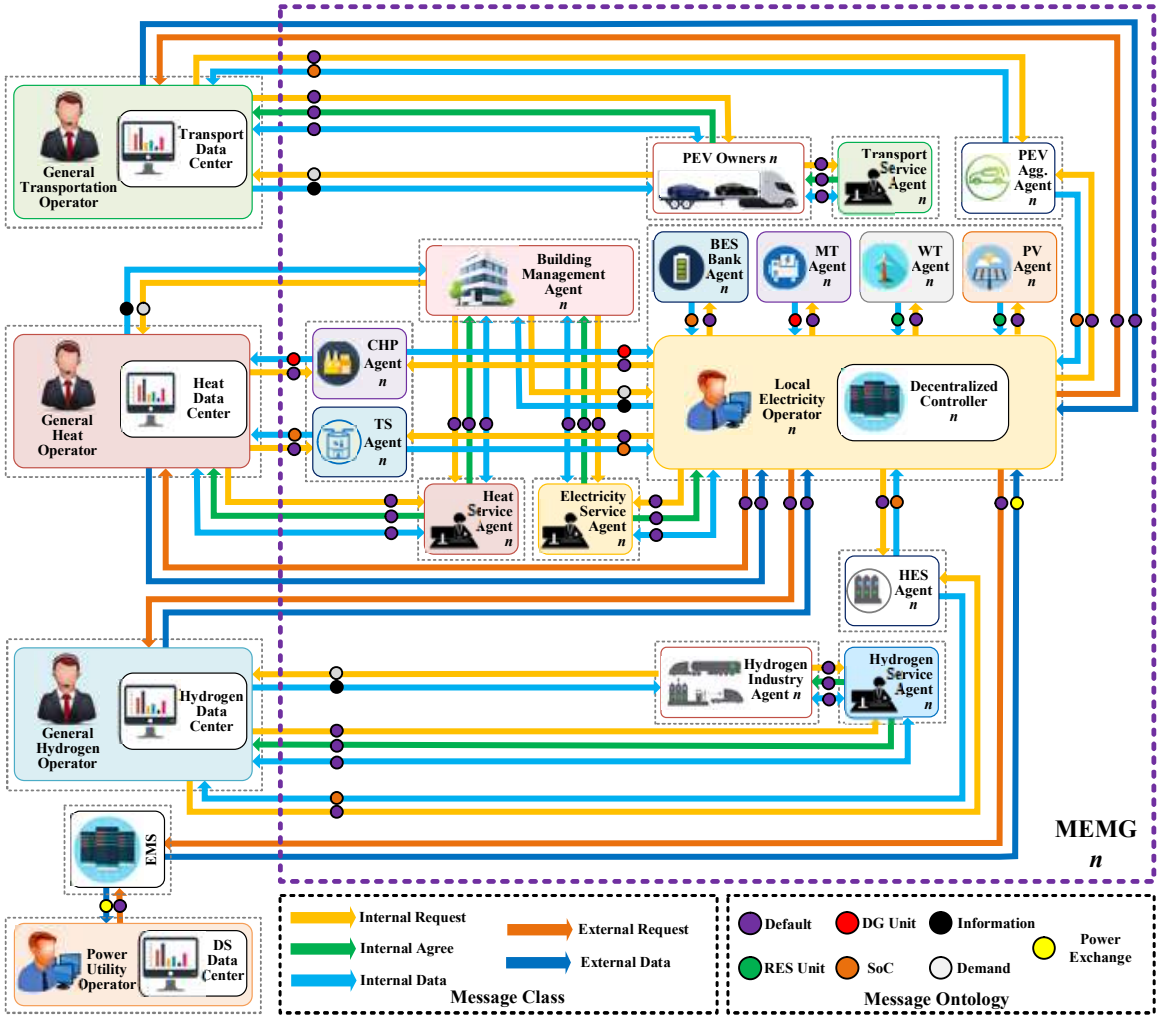

Figure 2: Proposed MAS-based analysis, communication network, and agent management ontology

1. **Local electricity operator** is a unit established for gathering and sharing required data, including real-time power prices and meteoric information with associated agents and other general energy operators. This unit acts as a local management agent that controls the power monitoring and real-time scheduling of each MEMG applying a decentralized controller to ensure the optimal operation.

2. **General energy operator** is established for determining and sharing required data, including real-time energy prices and operational constraints with the local electricity operator and other general energy operators. The general heat, transportation, and hydrogen operators perform as the management agent that controls the heat, transportation and hydrogen energy monitoring of each MEMG.
3. **Central EMS** is established for sharing required data, including updated penalty prices with local electricity operators in each MEMG. The central EMS performs as an independent entity that converge the power exchanges among the networked MEMGs in the decentralized framework and verifies whether the agreement among MEMGs concludes with the current penalty price.
4. **Energy consumer agent** collects relevant data about residential, commercial, and industrial tasks operating statuses, consumption demands, and signals of the system. Also. it sends required control commands back to the controllable devices to determine solutions for diverse consumer's objectives considering energy efficiency and a convenient life-form.
5. **Renewable energy supplier agent** gathers the meteorological data, forecasts the renewable energy generations in short-time periods and shares corresponding data to the requesting agent, i.e. local electricity operator. Since two kinds of renewable units, including WT and PV, are taken into account in the proposed analysis, two kinds of renewable energy supplier agents are developed as WT-agent and PV-agent.
6. **Fuel-based energy supplier agent** gathers the fuel cost data and shares them with the requesting agent, i.e. local electricity operator. Since two kinds of fuel-based units, including MT and CHP, are considered in the proposed examination, two kinds of fuel-based energy supplier agents are developed as MT-agent and CHP-agent.
7. **Energy storage agent** is developed to regulate the charge/discharge states of feasible energy storages. Since three kinds of energy storages, including BES, TES and HES, are considered, thus, three kind of energy storage agents are developed as BES-agent, TES-agent, and HES-agent. Besides, the PEV

aggregator can be also considered as the energy storage agent due to the charging/discharging behavior in the networked MEMGs.

8. **Energy service agent** assists other agents with particular kinds of computation services, e.g. required optimization algorithms. Such easy-response agent collects essential data as input and shares the optimal outputs of the system. In the proposed approach, the electricity, heat, transportation, and hydrogen service agents are designed.

It can be mentioned that in the presented MAS-based analysis, agents act collaboratively for attaining objectives such as supplying the energy demands of each MEMG continuously and maximizing the network total profit. Within the exploration, various ontologies are proposed and applied as references to ensure meaning to symbols in the message theme. Also, these ontologies facilitate identifying types of information to be applied in the sharing of messages, while verifying the data to be converted from the semantic point of view.

2.2. Decentralized Bi-Level Stochastic Optimization Approach

Communicating variables in the decentralized approach are generally the energy exchanges among the networked MEMGs. Each self-sufficient entity has its decision variables and intentions [40]. The proposed novel bi-level optimization approach in this paper is based on the modified progressive hedging (PH) algorithm as a heuristic algorithm to efficiently solve stochastic mixed-integer optimization problems with bounds on solution quality by penalizing constraint deviations in the objective function. The proposed algorithm can be implemented to acquire a feasible adjustment to the primary optimization problem, which also determines an upper bound on the optimal objective function merit and alleviate the computational complexity by disintegrating the optimization problem into scenario-based subproblems and solving them in parallel [41]. Accordingly, the penalty is contributed to the objective function of each scenario to converge the first level results of all generated scenarios to the same point. However, in this paper, the optimization problem is disintegrated based on the self-sufficient MAS-based networked MEMGs scheduling instead of scenario-based subproblems. This means that each MEMG has its

own optimal decisions. Hence, the exchanged energy among the MEMGs is modeled applying a stochastic decentralized bi-level optimization strategy. When both levels converge, the electrical power exchanges among the MEMGs are determined. It can be noted that this algorithm is fully adaptable for the reconfigurations and grid topologies. Figure 3 illustrates the flowchart of the proposed algorithm. The full operation steps can be figured out as follows.

Step 1: Define input parameters including capacity and hourly forecasted value of renewable unit, MT generation data, CHP unit data, characteristic of the TES, PEV aggregator data, HES data, hourly forecasted amount of active power, reactive power, and heat demands, hourly forecasted values of market prices.

Step 2: Generating problem scenarios for renewable units, active power, reactive power, and heat consumptions, and driving requirement of PEVs using the LHS method. More details about the LHS strategy are presented in Section 3.

Step 3: Reducing the number of generated scenarios to desired scenarios in GAMS software to enhance the calculation speed while sustaining the solution accuracy More details about the scenario reduction algorithm are described in Section 3.

Step 4: Solve the deterministic optimization problem for configured MEMGs to obtain the initial value for power exchange prices, $\mu^{\text{exchange}}_{(l,t)}$.

Step 5: Define the initial values for the electrical power exchanges and the corresponding penalty price at the running time of the optimization problem, t^{run}, as well as Equating the $\lambda_{(t,\beta)}$ and $P^{EX}_{(l,t,s)}$ with zero for all operating hours and scenarios.

Step 6: Solve the stochastic optimization problem of MEMG m in networked structure for t= $\{t^{\text{run}}, t^{\text{run}}+1, \cdots, t^{\text{schedule}}\}$ to obtain the power exchange value with the main grid, CHP units, PEV aggregators, and HES outputs for t= t^{run} as the results of the energy agents in this hour and set the calculated results as the input parameters for the optimization problem in Step 7.

Step 7: Solve the stochastic optimization problem of MEMG m in networked structure for t= t^{run} to obtain active and reactive power outputs of MTs, $\chi^{UP}_{(l,t,s,\alpha,\beta)}$ and $\chi^{DO}_{(l,t,s,\alpha,\beta)}$ as the results of electrical agents. $\chi^{UP}_{(l,t,s,\alpha,\beta)}$ and $\chi^{DO}_{(l,t,s,\alpha,\beta)}$ indicate the power exchange adjusted by the MEMG m from tie-line l at hour t for scenario s. The optimization problem is solved with the $\hat{\chi}^{UP}_{(l,t,s,\alpha-1,\beta)}$ and $\hat{\chi}^{DO}_{(l,t,s,\alpha-1,\beta)}$ to obtain $\chi^{UP}_{(l,t,s,\alpha,\beta)}$ and $\chi^{DO}_{(l,t,s,\alpha,\beta)}$. $\chi^{UP}_{(l,t,s,\alpha,\beta)}$ and $\chi^{DO}_{(l,t,s,\alpha,\beta)}$ indicate the power exchange adjusted by the neighboring MEMG connected to the MEMG m in the preceding first level iteration.

Step 8: Equate the decision-making variables of exchanged power, $P^{EX,\,UP}_{(l,t,s)}$ and $P^{EX,\,DO}_{(l,t,s)}$, with the adjusted electrical power exchange among networked MEMGs at hour t. In this case, the dependence of the decision-making variable at the two-level optimization problem on the adjusted operational value is removed. Furthermore, Equate the resulted decision-making variable of active and reactive power outputs of MTs, $P^{MT}_{(g,t,s)}$ and $Q^{MT}_{(g,t,s)}$, with the additional adjusted active and reactive power outputs of the MTs at hour t, $\pi^{MT}_{(g,t-1,s)}$ and $\theta^{MT}_{(g,t-1,s)}$. Accordingly, the value of the MT output at hour t can be preserved as a parameter in the optimization problem to ensure that the value of the generation ramp-rates of MTs between hours t and t-1 be in their allowed capacity limits.

Step 9: Investigate the first level convergence as as shown in Eq. (1).

$$\begin{matrix} \left|\chi^{UP}_{(l,t,s,\alpha,\beta)} - \chi^{UP}_{(l,t,s,\alpha-1,\beta)}\right| \leqslant \delta_1 \\ \left|\chi^{DO}_{(l,t,s,\alpha,\beta)} - \chi^{DO}_{(l,t,s,\alpha-1,\beta)}\right| \leqslant \delta_1 \end{matrix} \quad ; \quad \forall l, t, s \tag{1}$$

The first level convergence investigates whether the agreement among the networked MEMGs concludes with the present penalty price, the algorithm bounds back to Step 7 if it is not converged. It should be noted that it is not required to investigate the convergence of the power exchange adjusted by the neighboring MEMG connected to the MEMG m, $\hat{\chi}^{UP}_{(l,t,s,\alpha,\beta)}$ and $\hat{\chi}^{DO}_{(l,t,s,\alpha,\beta)}$, besides as a result of investigating the convergence of $\chi^{UP}_{(l,t,s,\alpha,\beta)}$ and $\chi^{DO}_{(l,t,s,\alpha,\beta)}$ for the related MEMG in the first level.

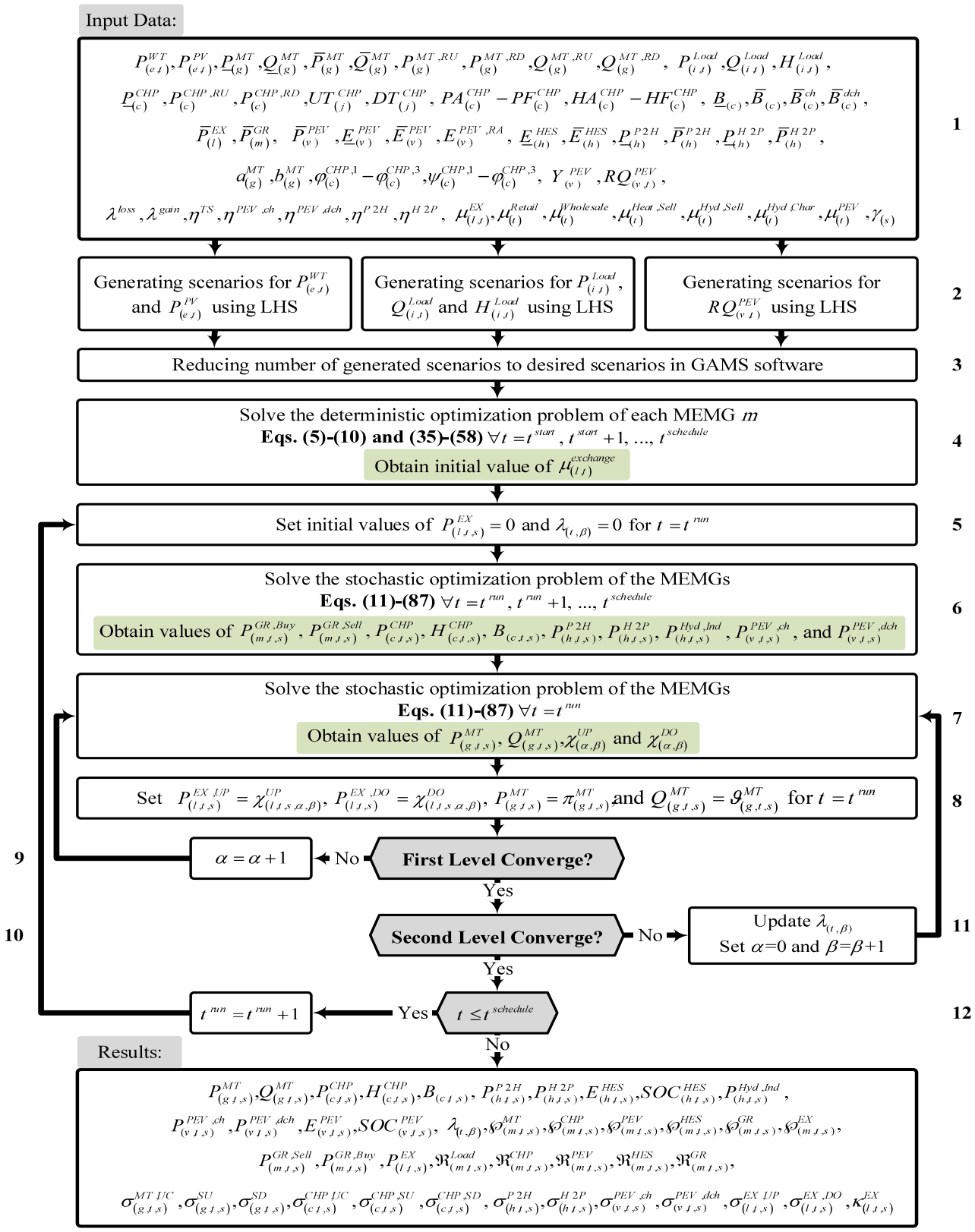

Figure 3: Flowchart of the proposed bi-level decentralized stochastic optimization problem

Step 10: Investigate the second level convergence as indicated by Eq. (2).

$$\begin{matrix} \left|\chi^{UP}_{(l,t,s,\alpha,\beta)} - \hat{\chi}^{DO}_{(l,t,s,\alpha,\beta)}\right| \leqslant \delta_2 \\ \left|\chi^{DO}_{(l,t,s,\alpha,\beta)} - \hat{\chi}^{UP}_{(l,t,s,\alpha,\beta)}\right| \leqslant \delta_2 \end{matrix} \quad ; \quad \forall l, t, s \tag{2}$$

Obviously, the second level convergence investigates whether the agreement among the networked MEMGs is achieved, the algorithm goes to Step 11 if it is not converged.

Step 11: Update the penalty price, $\lambda_{(t,\beta)}$, and bounds back to Step 7. More information about the proposed penalty price is represented in Section 3.

Step 12: Finally, the algorithm continues until the last scheduling time, $t^{schedule}$.

3. Proposed Formulation

The model of decentralized energy management and the corresponding local stochastic optimization problem of MEMG m are discussed in this section. Besides, a new pricing model is recommended for the initial power exchanges.

3.1. Model of Uncertainty

In this paper, multiple scenarios of renewable generations, active/reactive power and heat consumptions, and distance requirement of PEVs are generated presenting the Latin hypercube sampling (LHS) to realize the corresponding errors of forecasted values in a 24-hour scheduling interval. The LHS strategy indicates several conveniences including accelerating problem solutions and advanced sampling efficiency compared to the traditional Monte Carlo Simulation (MCS) approach [42]. The LHS will sustain the desired distributional properties while the sample volume expands during the investigation [43]. With many sampling-based numerical investigations for uncertainty analysis, it has been illustrated that the LHS strategy has various conveniences over the one-stage sampling strategies, particularly concerning improved convergence of the corresponding analysis and the robustness of the results to sampling variations. Even for reasonable numbers of iterations, the LHS strategy makes all or almost all sample means fall within a minor fraction of the standard error. When multiple simulations are performed, their means will be

much closer together with LHS than with MCS. This is how the LHS strategy makes simulations converge faster than MCS. Therefore, the LHS strategy is implemented to generate samples of renewable generations, demand fluctuations, and distance requirement of driving [44].

The LHS uncertainty approach can be assigned to the bi-stage method including the sampling stage and combination stage. In this paper, 1000 samples were generated to take into account the probabilistic characteristic of the renewable generations, load consumptions, and distance requirement of PEVs in the sampling stage. Consequently, the Cumulative Distribution Function (CDF) of the uncertain parameters is apportioned into 1000 portions with an equivalent probability of 1/1000. Hence, the following approach can be suggested for each generated scenario-based variable, as illustrated in Figure 4.

For k=1 to 1000:

Step 1: A value is randomly appointed from each portion. The illustrative probability of the CDF at portion k^{th} can be determined according to Eq. (3).

$$\mathrm{prob}_k = \frac{1}{1000}\left(\mathrm{rnd}_u + k - 1\right) \tag{3}$$

where, $\mathrm{rnd}_u \in (0,1)$ is a constantly distributed random weight.

Step 2: Eq. (4) expresses that the illustrative value is regularly adjusted into γ_k applying the inverse of distribution function F^{-1}:

$$\gamma_k = F^{-1}\left(\mathrm{prob}_k\right) \tag{4}$$

End For

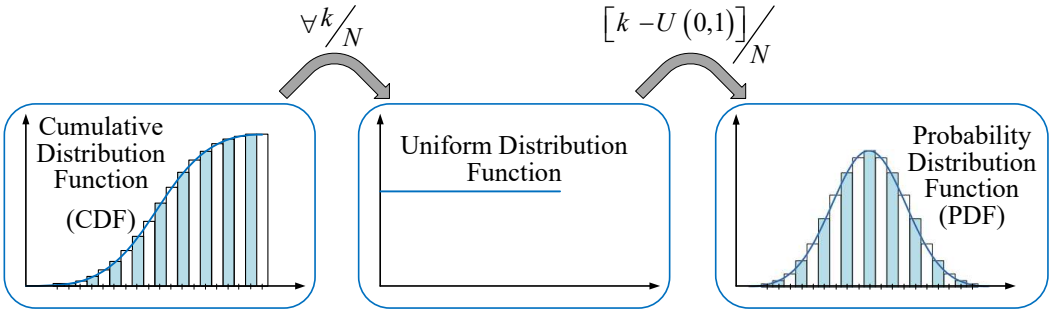

Figure 4: Uncertainty approach applying Latin Hypercube sampling

To provide the lowest correlation coefficients within the decision-making variables, the Cholesky factorization strategy is also adopted to merge the sampled values of the uncertain parameters. Besides, a backward scenario reduction technique is also applied in the bi-level stochastic optimization problem to reduce the number of scenarios and enhance the calculation speed [45].

3.2. Modeling of Power Exchange Prices

As mentioned previously, the e-MP and penalty function have been applied to the model for calculating the power exchange and penalty prices, respectively. Initially, the definition and some principles of the e-MP are reviewed. Then, the proposed e-MP model and method of calculating the power exchange prices are explained. Finally, the proposed penalty function is formulated by updating the relevant coefficient in the bi-level optimization approach.

3.2.1. Electrical Marginal Prices of MEMGs

The concept of the e-MP is derived from the definition of the Locational Marginal Price (LMP). However, in the concept of decentralized energy management, each MEMG is modeled as a self-sufficient agent to optimize its operational objectives. Accordingly, despite the interregional trading, the independent operation of each MEMG has made it realizable for marginal prices to be distinct in local MEMGs. In this proposed approach, to formulate the e-MP of MEMG m, it is assumed that the local power generation units and power consumptions are accumulated at a local node, and each MEMG is operated in the islanded mode applying the linear programming approach to reduce the complexity of the proposed model. It should be noted that power losses are ignored in the pricing model and only electrical energy agents are considered. Also, it is assumed that the price of selling electrical energy to consumers is equivalent to the price of generating electrical energy in each MEMG. The objective function of the MEMG operation problem is maximizing the cost function of the selling electrical energy, while it minimizes the cost function of generating electrical energy. Consequently, a convenient optimization problem for the proposed model can be formulated by Eqs. (5)-(8),

$$\min \quad FD_{(m,t)}(P^{Net,Load}_{(m,t)}) - FG_{(m,t)}(P^{Net,Generation}_{(m,t)}) \tag{5}$$

$$P^{Net,Load}_{(m,t)} - P^{Net,Generation}_{(m,t)} = 0 \tag{6}$$

$$P^{Net,Generation}_{(m,t)} = \sum_{g \in G_m} P^{MT}_{(g,t)} + \sum_{c \in C_m} P^{CHP}_{(c,t)} \tag{7}$$

$$P^{Net,Load}_{(m,t)} = \sum_{i \in I_m} P^{Load}_{(i,t)} - \sum_{e \in E_m} \left[P^{WT}_{(e,t)} + P^{PV}_{(e,t)} \right] \tag{8}$$

The result of the Lagrangian function of the above problem is defined in Eq. (9). $\tau_{(m,t)}$ represents the Lagrangian multiplier.

$$\frac{dFD_{(m,t)}}{dP^{Net,Load}_{(m,t)}} = \frac{dFG_{(m,t)}}{dP^{Net,Generation}_{(m,t)}} = \tau_{(m,t)} \tag{9}$$

The calculated value $\tau_{(m,t)}$ can be introduced as the e-MP of the MEMG m at hour t. As noted earlier, the initial price of power exchange among MEMG m and MEMG n through the tie-line l is regulated in regards to their e-MP. The proposed calculation can be simplified by Eq. (10). ϖ represents the weighted multiplier for regulating offered power exchange price.

$$\mu^{EX}_{(l,t)} = \frac{\varpi}{2} \left[\tau_{(m,t)} + \tau_{(n,t)} \right] \tag{10}$$

This multiplier can be selected as a number in the range of 1.5-2.5 under the operating conditions [46].

3.2.2. Penalty Function of Power Exchanges

In the proposed approach, only the electrical power is exchanged among the MEMGs through the tie-lines. For modeling the correlative impacts of operating conditions between the networked MEMGs, it is imperative to assign a penalty function in the agreement procedure of the proposed algorithm. Therefore, the penalty function can be defined in the form of Eq. (11). $\lambda_{(t,\beta)}$ represents the penalty price at hour t in the second-level iteration β.

$$\Delta^{EX}_{(l,t,s)} = \lambda_{(t,\beta)} \left[\frac{\chi^{UP}_{(l,t,s,\alpha,\beta)} - \hat{\chi}^{DO}_{(l,t,s,\alpha,\beta)}}{sgn\left(\chi^{UP}_{(l,t,s,\alpha,\beta)} - \hat{\chi}^{DO}_{(l,t,s,\alpha,\beta)}\right)} + \frac{\chi^{DO}_{(l,t,s,\alpha,\beta)} - \hat{\chi}^{UP}_{(l,t,s,\alpha,\beta)}}{sgn\left(\chi^{DO}_{(l,t,s,\alpha,\beta)} - \hat{\chi}^{UP}_{(l,t,s,\alpha,\beta)}\right)} \right] \tag{11}$$

The proposed penalty price is updated in each iteration β based on the regulation defined in Eq. (12). TL represents number of tie-lines in the MEMGs. Notably, this

number can be variant according to the network topology. Cleary, higher z value represents a stricter penalty price and may result in the optimum decisions, while a lower z value represents that more iterations are desired for the convergence of the agreed power exchanges between the MEMGs. It is obvious that the penalty price is rising until the power exchanges agreed by the neighboring MEMGs reach an equal value.

$$\lambda_{(t,\beta)} = \lambda_{(t,\beta-1)} + \frac{1}{z}\left(\frac{1}{TL}\sum_{l}\mu^{EX}_{(l,t)}\right) \tag{12}$$

3.3. Objective Function of the Proposed Stochastic Optimization Problem

The decentralized controller of the MEMG schedules the energy resources in such a way that the total profit of the MEMG is maximized. The objective function of the proposed stochastic optimization problem of the local MAS-based MEMG m from the networked structure point of view can be formulated by Eq. (13). I_m, G_m, C_m, E_m, V_m, H_m, and L_m are sets of loads, MTs, CHP units and TESs, renewable units, PEV aggregators, HESs and tie-lines in MEMG m.

$$\max \quad \text{Profit}_{(m)} = \sum_t \sum_s \gamma_{(s)} \left[\begin{array}{l} \left(\Re^{Load}_{(m,t,s)} + \Re^{CHP}_{(m,t,s)} + \Re^{PEV}_{(m,t,s)} + \Re^{HES}_{(m,t,s)}\right) - \\ \left(\wp^{MT}_{(m,t,s)} + \wp^{CHP}_{(m,t,s)} + \wp^{PEV}_{(m,t,s)} + \wp^{HES}_{(m,t,s)}\right) + \\ \left(\Re^{GR}_{(m,t,s)} - \wp^{GR}_{(m,t,s)}\right) + \left(\wp^{EX}_{(m,t,s)} + \Delta^{EX}_{(l,s)}\right) \end{array} \right] \tag{13}$$

$$\Re^{Load}_{(m,t,s)} = \sum_{I_m} \mu^{Retail}_{(t)}.P^{Load}_{(i,t,s)}; \quad \forall m,t,s \tag{14}$$

$$\Re^{CHP}_{(m,t,s)} = \sum_{I_m} \mu^{Heat,Sell}_{(t)}.H^{Load}_{(i,t,s)}; \quad \forall m,t,s \tag{15}$$

$$\Re^{PEV}_{(m,t,s)} = \sum_{V_m} \mu^{Retail}_{(t)}.Y^{PEV}_{(v)}.RQ^{PEV}_{(v,t)}; \quad \forall m,t,s \tag{16}$$

$$\Re^{HES}_{(m,t,s)} = \sum_{H_m} \mu^{Hyd,Sell}_{(t)}.P^{Hyd,Ind}_{(h,t,s)}; \quad \forall m,t,s \tag{17}$$

$$\wp^{MT}_{(m,t,s)} = \sum_{G_m} \left[a^{MT}_{(g)}.P^{MT}_{(g,t,s)} + b^{MT}_{(g)}.\sigma^{MT,UC}_{(g,t,s)}\right] \; ; \quad \forall m,t,s \tag{18}$$

$$\wp^{CHP}_{(m,t,s)} = \sum_{C_m} \left[\begin{array}{l} \varphi^{CHP,1}_{(c)}.\left(P^{CHP}_{(c,t,s)}\right)^2 + \varphi^{CHP,2}_{(c)}.P^{CHP}_{(c,t,s)} + \varphi^{CHP,3}_{(c)} + \\ \psi^{CHP,1}_{(c)}.\left(H^{CHP}_{(c,t,s)}\right)^2 + \psi^{CHP,2}_{(c)}.H^{CHP}_{(c,t,s)} + \psi^{CHP,3}_{(c)} \end{array} \right] \; ; \quad \forall m,t,s \tag{19}$$

$$\wp^{PEV}_{(m,t,s)} = \sum_{V_m} \mu^{PEV}_{(t)} . \left[\eta^{PEV,ch} . P^{PEV,ch}_{(v,t,s)} - \left(1/\eta^{PEV,dch}\right) . P^{PEV,dch}_{(v,t,s)} \right]; \quad \forall m, t, s \tag{20}$$

$$\wp^{HES}_{(m,t,s)} = \sum_{H_m} \mu^{Hyd,Char}_{(t)} . P^{P2H}_{(h,t,s)}; \quad \forall m, t, s \tag{21}$$

$$\Re^{GR}_{(m,t,s)} = \mu^{Wholesale}_{(t)} . P^{GR,Sell}_{(m,t,s)}; \quad \forall m, t, s \tag{22}$$

$$\wp^{GR}_{(m,t,s)} = \mu^{Wholesale}_{(t)} . P^{GR,Buy}_{(m,t,s)}; \quad \forall m, t, s \tag{23}$$

$$\wp^{EX}_{(m,t,s)} = \sum_{L_m} \mu^{EX}_{(l,t)} . P^{EX}_{(l,t,s)}; \quad \forall m, t, s \tag{24}$$

In the objective function presented by Eq. (13), the first and the second parentheses indicate the revenue and operational cost functions of the MEMG m, respectively, which are performed by scheduling different energy sources. The first term of the MEMG revenue is gained by selling electrical energy to the electrical consumers owing to retail market price signals. The second term is related to selling heat energy generated by the CHP units to the heat consumers owing to heat price signals. The third term is related to selling electrical energy to the PEV aggregators for providing driving requirements. The fourth term denotes the benefit of exporting hydrogen energy to the hydrogen industry. The fifth and sixth terms are related to the MEMG operational costs of generated electrical and heat energies in MT and CHP units, respectively. Seventh term indicates costs related to the charging and discharging power of the PEV aggregators. The eighth term is associated with the charging cost of HESs. The nineth and tenth terms of Eq. (13) demonstrate the MEMG revenue gained by selling electrical energy to the main grid and operating costs related to buying electrical energy from the main grid, respectively, owing to wholesale market price signals. The eleventh term shows the costs of electrical energy exchanges between the MEMG m and neighboring MEMGs through tie-lines. The twelfth term demonstrates the cost function of the penalty price for regulating the value of the converged power exchanges. The revenue functions corresponding to the energy demanded by the electrical consumers, heat consumers, PEV aggregators, and hydrogen industry are modeled by Eqs. (14)-(17), respectively. Also, the cost functions corresponding to the energy provided by the MTs, CHP units, PEV aggregators, and HESs are modeled by Eqs. (18)-(21), respectively. The functions corresponding to sell and buy electrical energy from the main grid can be also

modeled by Eqs. (22) and (23), respectively. Furthermore, the cost of exchanging electrical energy is formulated by Eq. (24).

3.4. Constraints

The constraints of the stochastic optimization problem of the MAS-based networked MEMGs can be presented as Eqs. (29) and (87).

3.4.1. Distribution Power Flow

The constraints presented by Eqs. (25)-(28) are the linear Dist. Flow equations of power distribution networks which describe the power flow at each node i [47].

$$\begin{aligned} P^{Flow}_{(i+1,t,s)} = P^{Flow}_{(i,t,s)} + P^{MT}_{(g,t,s)} + P^{WT}_{(e,t,s)} + P^{PV}_{(e,t,s)} \\ + P^{CHP}_{(c,t,s)} + P^{H2P}_{(h,t,s)} - P^{P2H}_{(h,t,s)} \\ + P^{PEV,dch}_{(v,t,s)} - P^{PEV,ch}_{(v,t,s)} - P^{Load}_{(i,t,s)} \;\; ; \quad \forall i,t,s \end{aligned} \tag{25}$$

$$Q^{Flow}_{(i+1,t,s)} = Q^{Flow}_{(i,t,s)} + Q^{MT}_{(g,t,s)} - Q^{Load}_{(i,t,s)} \;\; ; \quad \forall i,t,s \tag{26}$$

$$v_{(i+1,t,s)} = v_{(i,t,s)} - 2\left[r_{(i)}.P^{Flow}_{(i,t,s)} + x_{(i)}.Q^{Flow}_{(i,t,s)}\right] \;\; ; \quad \forall i,t,s \tag{27}$$

$$(1-\epsilon)^2 \leqslant v_{(i,t,s)} \leqslant (1+\epsilon)^2 \;\; ; \quad v_{(i,t,s)} = \left|V_{(i,t,s)}\right|^2 \;\; ; \quad \forall i,t,s \tag{28}$$

3.4.2. Constraints of Power Exchange with other MEMGs

To deal with the complex application of bi-directional energy transactions between the MEMGs, the associated power exchange variable is transformed into two additional positive variables with diverse power exchange directions as demonstrated in Eqs. (29)-(31). Consequently, an energy transaction status and the status of the implemented tie-line switches are addressed for each active power exchange variable to prevent bidirectional exchange simultaneously at hour t (Eq. (32)).

$$-\overline{P}^{EX}_{(l)}.\kappa^{EX}_{(l)}.\sigma^{EX,UP}_{(l,t,s)} \leqslant P^{EX,UP}_{(l,t,s)} \leqslant \overline{P}^{EX}_{(l)}.\kappa^{EX}_{(l)}.\sigma^{EX,UP}_{(l,t,s)} \;\; ; \quad \forall l,t,s \tag{29}$$

$$-\overline{P}^{EX}_{(l)}.\kappa^{EX}_{(l)}.\sigma^{EX,DO}_{(l,t,s)} \leqslant P^{EX,DO}_{(l,t,s)} \leqslant \overline{P}^{EX}_{(l)}.\kappa^{EX}_{(l)}.\sigma^{EX,DO}_{(l,t,s)} \;\; ; \quad \forall l,t,s \tag{30}$$

$$P^{EX}_{(l,t,s)} = P^{EX,UP}_{(l,t,s)} + P^{EX,DO}_{(l,t,s)} \;\; ; \quad \forall l,t,s \tag{31}$$

$$\sigma^{EX,UP}_{(l,t,s)} + \sigma^{EX,DO}_{(l,t,s)} < 1 \;\; ; \quad \forall l,t,s \tag{32}$$

3.4.3. Constraints of Power Exchange with Main Grid

The power exchange between MEMG m and main grid should be limited to the capacity of transformers located in the substations (Eqs. (33) and (34)).

$$0 < P^{GR,Buy}_{(m,t,s)} < \overline{P}^{GR}_{(m)}; \quad \forall m, s, t \tag{33}$$

$$0 < P^{GR,Sell}_{(m,t,s)} < \overline{P}^{GR}_{(m)}; \quad \forall m, s, t \tag{34}$$

3.4.4. MT Constraints

The constraints demonstrated by Eqs. (35)-(42) guarantee that an MT output value is in its generation capacity. The allowed generation limits compounded with commitment states, up/down ramp-rate boundaries, and start-up/shot-down states are incorporated as the MT constraints.

$$\underline{P}^{MT}_{(g)}.\sigma^{MT,UC}_{(g,t,s)} \leqslant P^{MT}_{(g,t,s)} \leqslant \overline{P}^{MT}_{(g)}.\sigma^{MT,UC}_{(g,t,s)} \quad ; \quad \forall g, t, s \tag{35}$$

$$\pi^{MT}_{(g,t-1,s)} - P^{MT}_{(g,t,s)} = P^{MT,RU}_{(g)}.\left[1 - \sigma^{SU}_{(g,t,s)}\right] \quad ; \quad \forall g, t, s \tag{36}$$

$$P^{MT}_{(g,t,s)} - \pi^{MT}_{(g,t-1,s)} = P^{MT,RD}_{(g)}.\left[1 - \sigma^{SD}_{(g,t,s)}\right] \quad ; \quad \forall g, t, s \tag{37}$$

$$\underline{Q}^{MT}_{(g)}.\sigma^{MT,UC}_{(g,t,s)} \leqslant Q^{MT}_{(g,t,s)} \leqslant \overline{Q}^{MT}_{(g)}.\sigma^{MT,UC}_{(g,t,s)} \quad ; \quad \forall g, t, s \tag{38}$$

$$\theta^{MT}_{(g,t-1,s)} - Q^{MT}_{(g,t,s)} = Q^{MT,RU}_{(g)}.\left[1 - \sigma^{SU}_{(g,t,s)}\right] \quad ; \quad \forall g, t, s \tag{39}$$

$$Q^{MT}_{(g,t,s)} - \theta^{MT}_{(g,t-1,s)} = Q^{MT,RD}_{(g)}.\left[1 - \sigma^{SD}_{(g,t,s)}\right] \quad ; \quad \forall g, t, s \tag{40}$$

$$\sigma^{SU}_{(g,t,s)} + \sigma^{SD}_{(g,t,s)} < 1 \quad ; \quad \forall g, t, s \tag{41}$$

$$\sigma^{SU}_{(g,t,s)} - \sigma^{SD}_{(g,t,s)} - \sigma^{UC}_{(g,t,s)} + \sigma^{UC}_{(g,t-1,s)} = 0 \quad ; \quad \forall g, t, s \tag{42}$$

3.4.5. CHP Unit Constraints

The power and heat generations of CHP units are interdependent and cannot operate individually. Based on the Ref. [48], two types of scheduling regions can be defined for CHP units which are illustrated in Figure 5.

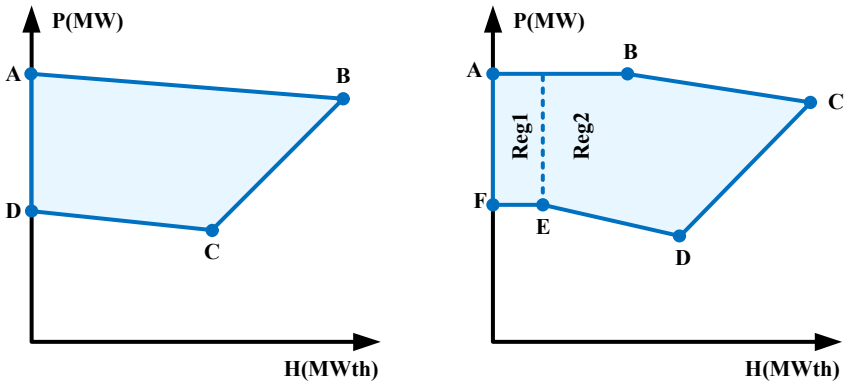

(a) Type 1 (b) Type 2

Figure 5: Heat-power feasible operation region of CHP units, (a) type 1, (b) type 2

The first type of scheduling region of CHP units can be defined in a linear model as Eqs. (43)-(47). Eq. (43) indicates the region under the line AB. Also, the upper region of line BC and line CD are expressed by Eqs. (44) and (45), respectively. Furthermore, the upper heat and power generation limits of the CHP unit are bounded by Eqs. (46) and (47), respectively.

$$P^{CHP}_{(c,t,s)} - PA^{CHP}_{(c)} - \frac{PA^{CHP}_{(c)} - PB^{CHP}_{(c)}}{HA^{CHP}_{(c)} - HB^{CHP}_{(c)}} \left[H^{CHP}_{(c,t,s)} - HA^{CHP}_{(c)}\right] \leqslant 0; \quad \forall c, t, s \tag{43}$$

$$P^{CHP}_{(c,t,s)} - PB^{CHP}_{(c)} - \frac{PB^{CHP}_{(c)} - PC^{CHP}_{(c)}}{HB^{CHP}_{(c)} - HC^{CHP}_{(c)}} \left[H^{CHP}_{(c,t,s)} - HB^{CHP}_{(c)}\right] \geqslant -\left(1 - \sigma^{CHP,UC}_{(c,t,s)}\right) M; \quad \forall c, t, s \tag{44}$$

$$P^{CHP}_{(c,t,s)} - PC^{CHP}_{(c)} - \frac{PC^{CHP}_{(c)} - PD^{CHP}_{(c)}}{HC^{CHP}_{(c)} - HD^{CHP}_{(c)}} \left[H^{CHP}_{(c,t,s)} - HC^{CHP}_{(c)}\right] \geqslant -\left(1 - \sigma^{CHP,UC}_{(c,t,s)}\right) M; \quad \forall c, t, s \tag{45}$$

$$0 \leqslant H^{CHP}_{(c,t,s)} \leqslant HB^{CHP}_{(c)}.\sigma^{CHP,UC}_{(c,t,s)}; \quad \forall c, t, s \tag{46}$$

$$0 \leqslant P^{CHP}_{(c,t,s)} \leqslant PA^{CHP}_{(c)}.\sigma^{CHP,UC}_{(c,t,s)}; \quad \forall c, t, s \tag{47}$$

In order to formulate the second type of scheduling region for CHP units (Figure 5(b)) in a linear model, heat-power feasible operation region is apportioned into

two main sub-regions I and II applying two additional binary variables ($\sigma^{CHP,R2}_{(c,t,s)}$/ $\sigma^{CHP,R1}_{(c,t,s)}$). Equation (48) indicates the region under the line BC. Also, the upper region of the lines CD, DE, and EF are expressed by Eqs. (49)-(51), respectively. In Eqs. (50)-(53), $\sigma^{CHP,R1}_{(c,t,s)} = 1/\sigma^{CHP,R2}_{(c,t,s)} = 1$ implies CHP unit schedule in region I/II. Based on Eq. (55), the CHP unit can be scheduled either in the region I or II. Furthermore, the upper heat and power generation limits of the CHP unit are bounded by Eqs. (55) and (56), respectively.

$$P^{CHP}_{(c,t,s)} - PB^{CHP}_{(c)} - \frac{PB^{CHP}_{(c)} - PC^{CHP}_{(c)}}{HB^{CHP}_{(c)} - HC^{CHP}_{(c)}} \left[H^{CHP}_{(c,t,s)} - HB^{CHP}_{(c)}\right] \leqslant 0; \quad \forall c, t, s \tag{48}$$

$$P^{CHP}_{(c,t,s)} - PC^{CHP}_{(c)} - \frac{PC^{CHP}_{(c)} - PD^{CHP}_{(c)}}{HC^{CHP}_{(c)} - HD^{CHP}_{(c)}} \left[H^{CHP}_{(c,t,s)} - HC^{CHP}_{(c)}\right] \geqslant 0; \quad \forall c, t, s \tag{49}$$

$$P^{CHP}_{(c,t,s)} - PE^{CHP}_{(c)} - \frac{PE^{CHP}_{(c)} - PF^{CHP}_{(c)}}{HE^{CHP}_{(c)} - HF^{CHP}_{(c)}} \left[H^{CHP}_{(c,t,s)} - HE^{CHP}_{(c)}\right] \geqslant -\left(1 - \sigma^{CHP,R1}_{(c,t,s)}\right) M; \quad \forall c, t, s \tag{50}$$

$$P^{CHP}_{(c,t,s)} - PD^{CHP}_{(c)} - \frac{PD^{CHP}_{(c)} - PE^{CHP}_{(c)}}{HD^{CHP}_{(c)} - HE^{CHP}_{(c)}} \left[H^{CHP}_{(c,t,s)} - HD^{CHP}_{(c)}\right] \geqslant -\left(1 - \sigma^{CHP,R2}_{(c,t,s)}\right) M; \quad \forall c, t, s \tag{51}$$

$$H^{CHP}_{(c,t,s)} - HE^{CHP}_{(c,t,s)} \leqslant -\left(1 - \sigma^{CHP,R1}_{(c,t,s)}\right) M; \quad \forall c, t, s \tag{52}$$

$$H^{CHP}_{(c,t,s)} - HE^{CHP}_{(c,t,s)} \geqslant -\left(1 - \sigma^{CHP,R2}_{(c,t,s)}\right) M; \quad \forall c, t, s \tag{53}$$

$$\sigma^{CHP,R1}_{(c,t,s)} + \sigma^{CHP,R2}_{(c,t,s)} = \sigma^{CHP,UC}_{(c,t,s)}; \quad \forall c, t, s \tag{54}$$

$$0 \leqslant H^{CHP}_{(c,t,s)} \leqslant HC^{CHP}_{(c)}.\sigma^{CHP,UC}_{(c,t,s)}; \quad \forall c, t, s \tag{55}$$

$$0 \leqslant P^{CHP}_{(c,t,s)} \leqslant PA^{CHP}_{(c)}.\sigma^{CHP,UC}_{(c,t,s)}; \quad \forall c, t, s \tag{56}$$

The start-up and shut-down expanses of CHP units are also presented by Eqs. (57) and (58), respectively.

$$SUC^{CHP}_{(c,t,s)} = SU^{CHP}_{(c)}.\sigma^{CHP,SU}_{(c,t,s)}; \quad \forall c, t, s \tag{57}$$

$$SDC^{CHP}_{(c,t,s)} = SD^{CHP}_{(c)}.\sigma^{CHP,SD}_{(c,t,s)}; \quad \forall c, t, s \tag{58}$$

Plus, the constraints of ramp-up, ramp-down, minimum down-time, and minimum up-time can be also presented by Eqs. (59)-(65):

$$P^{CHP}_{(c,t,s)} - P^{CHP}_{(c,t-1,s)} \leqslant P^{CHP,RU}_{(c)} \left(1 - \sigma^{CHP,SU}_{(c,t,s)}\right) + \underline{P}^{CHP}_{(c)}.\sigma^{CHP,SU}_{(c,t,s)}; \quad \forall c, t, s \tag{59}$$

$$P^{CHP}_{(c,t-1,s)} - P^{CHP}_{(c,t,s)} \leqslant P^{CHP,RD}_{(c)} \left(1 - \sigma^{CHP,SD}_{(c,t,s)}\right) + \underline{P}^{CHP}_{(c)}.\sigma^{CHP,SD}_{(c,t,s)}; \quad \forall c, t, s \tag{60}$$

$$\sum_{h=1}^{t+UT^{CHP}_{(j)}-1} \sigma^{CHP,UC}_{(j,h,s)} \geqslant UT^{CHP}_{(j)}.\sigma^{CHP,SU}_{(c,t,s)}; \quad \forall c, t, s \tag{61}$$

$$\sum_{h=1}^{t+DT^{CHP}_{(j)}-1} \left(1 - \sigma^{CHP,UC}_{(j,h,s)}\right) \geqslant DT^{CHP}_{(j)}.\sigma^{CHP,SD}_{(c,t,s)}; \quad \forall c, t, s \tag{62}$$

$$\sigma^{CHP,UC}_{(c,t+1,s)} - \sigma^{CHP,UC}_{(c,t,s)} \leqslant \sigma^{CHP,SU}_{(c,t+1,s)} \ ; \quad \forall c, t, s \tag{63}$$

$$\sigma^{CHP,UC}_{(c,t,s)} - \sigma^{CHP,UC}_{(c,t+1,s)} \leqslant \sigma^{CHP,SD}_{(c,t+1,s)} \ ; \quad \forall c, t, s \tag{64}$$

$$\sigma^{CHP,UC}_{(c,t+1,s)} - \sigma^{CHP,UC}_{(c,t,s)} \leqslant \sigma^{CHP,SU}_{(c,t+1,s)} - \sigma^{CHP,SD}_{(c,t+1,s)} \ ; \quad \forall c, t, s \tag{65}$$

3.4.6. TES Constraints

The TES system can be formulated based on the model presented in Ref. [49]. As the heat transferred with the TES is affected by the loss (λ^{loss}) and extra (λ^{gain}) heat generation during shutdown and startup times, the actual heat ($H_{(c,t,s)}$), can be formulated as Eq. (66).

$$H_{(c,t,s)} = \sum_{c=1}^{C_m} H^{CHP}_{(c,t,s)} - \lambda^{loss}.\sigma^{CHP,SU}_{(c,t+1,s)} + \lambda^{gain}.\sigma^{CHP,SD}_{(c,t+1,s)} \ ; \quad \forall c, t, s \tag{66}$$

The feasible heat in the TES ($B_{(c,t,s)}$) considering the TES efficiency (η^{TS}) can be formulated by Eq. (67).

$$B_{(c,t,s)} = \eta^{TS}.B_{(c,t-1,s)} + H_{(c,t,s)} - \sum_{i=1}^{H_m} H^{DE}_{(i,t,s)} \ ; \quad \forall c, t, s \tag{67}$$

Furthermore, the capacity of TES is bounded in Eq. (68). $\underline{B}_{(c)}$ and $\overline{B}_{(c)}$ are lower and upper thermal capacities of TESs, respectively.

$$\underline{B}_{(c)} \leqslant B_{(c,t,s)} \leqslant \overline{B}_{(c)} \ ; \quad \forall c, t, s \tag{68}$$

To simulate actual state of TES, ramp-up and ramp-down rates are also taken into account as Eqs. (69) and (70). $\overline{B}^{ch}_{(c)}$ and $\overline{B}^{dch}_{(c)}$ are the maximum allowed charge and discharge rates of TES, respectively.

$$B_{(c,t,s)} - B_{(c,t-1,s)} \leqslant \overline{B}^{ch}_{(c)} \;\; ; \quad \forall c, t, s \tag{69}$$

$$B_{(c,t-1,s)} - B_{(c,t,s)} \leqslant \overline{B}^{dch}_{(c)} \;\; ; \quad \forall c, t, s \tag{70}$$

3.4.7. HES Constraints

The level of hydrogen stored in the HES at time t is defined by Eq. (71) and bounded by Eq. (72) due to the storage system potential. The HES, like the TES and BES, has some boundaries for charging and discharging modes. Eq. (73) shows the energy state of hydrogen stored in the HES at time t. Eq. (74) ensures that the amount of active power converted to the hydrogen energy is in its capacity boundaries. Similarly, Eq. (75) limits the amount of stored hydrogen energy converted to the active power. Also, Eq. (76) indicates that the active power cannot be converted to hydrogen energy and stored hydrogen cannot be converted to active power simultaneously.

$$E^{HES}_{(h,t,s)} = E^{HES}_{(h,t-1,s)} + \eta^{P2H}.P^{P2H}_{(h,t,s)} - \left(1/\eta^{H2P}\right) P^{H2P}_{(h,t,s)} - P^{Hyd,Ind}_{(h,t,s)} \;\; ; \quad \forall h, t, s \tag{71}$$

$$\underline{E}^{HES}_{(h)} \leqslant E^{HES}_{(h,t,s)} \leqslant \overline{E}^{HES}_{(h)} \;\; ; \quad \forall h, t, s \tag{72}$$

$$SOC^{HES}_{(h,t,s)} = E^{HES}_{(h,t,s)} / \overline{E}^{HES}_{(h)} \;\; ; \quad \forall h, t, s \tag{73}$$

$$\underline{P}^{P2H}_{(h)}.\sigma^{P2H}_{(h,t,s)} \leqslant P^{P2H}_{(h,t,s)} \leqslant \overline{P}^{P2H}_{(h)}.\sigma^{P2H}_{(h,t,s)} \;\; ; \quad \forall h, t, s \tag{74}$$

$$\underline{P}^{H2P}_{(h)}.\sigma^{H2P}_{(h,t,s)} \leqslant P^{H2P}_{(h,t,s)} \leqslant \overline{P}^{H2P}_{(h)}.\sigma^{H2P}_{(h,t,s)} \;\; ; \quad \forall h, t, s \tag{75}$$

$$\sigma^{P2H}_{(h,t,s)} + \sigma^{H2P}_{(h,t,s)} \leqslant 1 \;\; ; \quad \forall h, t, s \tag{76}$$

3.4.8. PEV Aggregator Constraints

The scheduling constraints for PEV aggregators are formulated by Eqs. (77)-(84). The energy balance of the PEV aggregators is presented by Eq. (77). Eq. (78) shows the energy state stored in the PEV at time t. Eqs. (79)-(81) indicated the upper/lower amount of charging/discharging of PEVs. Eq. (82) ensures that each PEV be in its energy storage capacity. Also, the amount of required stored energy to provide the driving requests is represented in Eq. (83). Furthermore, Eq. (84) guarantees the ramp rate value of charging/discharging of PEVs.

$$E^{PEV}_{(\nu,t,s)} = E^{PEV}_{(\nu,t-1,s)} + \eta^{PEV,ch}.P^{PEV,ch}_{(\nu,t,s)} - \left(1/\eta^{PEV,dch}\right).P^{PEV,dch}_{(\nu,t,s)} - Y^{PEV}_{(\nu)}.RQ^{PEV}_{(\nu,t)} \quad \forall \nu, t, s \tag{77}$$

$$SOC^{PEV}_{(h,t,s)} = E^{PEV}_{(h,t,s)} / \overline{E}^{PEV}_{(h)} \;\; ; \quad \forall \nu, t, s \tag{78}$$

$$0 \leqslant P^{PEV,ch}_{(\nu,t,s)} \leqslant \overline{P}^{PEV}_{(\nu)}.\sigma^{PEV,ch}_{(\nu,t,s)} \;\; ; \quad \forall \nu, t, s \tag{79}$$

$$0 \leqslant P^{PEV,dch}_{(\nu,t,s)} \leqslant \overline{P}^{PEV}_{(\nu)}.\sigma^{PEV,dch}_{(\nu,t,s)} \;\; ; \quad \forall \nu, t, s \tag{80}$$

$$\sigma^{PEV,ch}_{(\nu,t,s)} + \sigma^{PEV,dch}_{(\nu,t,s)} \leqslant 1 \;\; ; \quad \forall \nu, t, s \tag{81}$$

$$\underline{E}^{PEV}_{(\nu)} \leqslant E^{PEV}_{(\nu,t,s)} \leqslant \overline{E}^{PEV}_{(\nu)} \;\; ; \quad \forall \nu, t, s \tag{82}$$

$$E^{PEV}_{(\nu,t,s)} - \underline{E}^{PEV}_{(\nu)} \geqslant \eta^{PEV,dch}.Y^{PEV}_{(\nu)}.RQ^{PEV}_{(\nu,t)} \;\; ; \quad \forall \nu, t, s \tag{83}$$

$$E^{PEV}_{(\nu,t,s)} - E^{PEV}_{(\nu,t-1,s)} \leqslant E^{PEV,RA}_{(\nu)} \;\; ; \quad \forall \nu, t, s \tag{84}$$

3.4.9. Heat and Power Balance Constraints

To investigate the reliable decentralized energy management of MEMGs, the constraint of active power, reactive power, and heat balances between the total local generation and consumption in each MEMG is required per scenario and per hour of the scheduling period. Accordingly, the active power, reactive power, and heat balance constraints at MEMG m at hour t for scenario s can be respectively represented by Eqs. (85) and (87).

$$\begin{aligned} \textstyle\sum_{I_m} P^{Load}_{(i,t,s)} = {} & P^{Grid,Buy}_{(m,t,s)} - P^{Grid,Sell}_{(m,t,s)} \\ & + \textstyle\sum_{G_m} P^{MT}_{(g,t,s)} + \sum_{C_m} P^{CHP}_{(c,t,s)} \\ & + \textstyle\sum_{E_m} \left[P^{WT}_{(e,t,s)} + P^{PV}_{(e,t,s)}\right] \\ & + \textstyle\sum_{H_m} \left[P^{H2P}_{(h,t,s)} - P^{P2H}_{(h,t,s)}\right] \\ & + \textstyle\sum_{V_m} \left[P^{PEV,dch}_{(\nu,t,s)} - P^{PEV,ch}_{(\nu,t,s)}\right] \\ & + \textstyle\sum_{L_m} \left[P^{EX,UP}_{(l,t,s)} - P^{EX,DO}_{(l,t,s)}\right] \;\; ; \quad \forall m, t, s \end{aligned} \tag{85}$$

$$\sum_{I_m} Q^{Load}_{(i,t,s)} = \sum_{G_m} Q^{MT}_{(g,t,s)} \;\; ; \quad \forall m, t, s \tag{86}$$

$$\sum_{I_m} H^{Load}_{(i,t,s)} = \sum_{C_m} H^{CHP}_{(c,t,s)} \;\; ; \quad \forall m, t, s \tag{87}$$

4. Case Study Applications

In this paper, the derived model is simulated over a network with three MAS-based networked MEMGs as illustrated in Figure 6, and the total profit of each MEMG is maximized over a 24-hour time horizon operation in three different scheduling case studies to accurately investigate the performance of the proposed decentralized approach in the presence of multi-energy storages. Each MEMG includes the MTs as dispatchable DGs, renewable units as non-dispatchable DGs, CHP units, PEV aggregators, HESs, and active/reactive power and heat demands. The hourly forecasted multipliers of the renewable generations are illustrated in Figure 7. The hourly forecasted multipliers of active power, reactive power, and heat demands are illustrated in Figure 8. Also, the maximum active power, reactive power, and heat demands of each node in the network are assumed to be 1 MW, 0.4 MVAR, and 0.33 MWth, respectively. Furthermore, the forecasted values of the day-ahead electricity market prices, retail-rate prices, and heat prices are represented in Figure 9. Table 2 represents the installed capacity of renewable units containing wind turbines (WTs) and photovoltaic (PV) systems. Besides, Table 3 represents the location, as well as technical and economic data of MTs. The techno-economic data of the CHP units and the feasible operation region data of CHP units are also presented in Tables 4 and 5, respectively. Besides, the characteristics of the TES and the required data of PEV aggregator are respectively presented in Tables 6 and 7. The location and data of HESs are shown in Table 8. Figure 10 illustrate the driving requirement pattern of each PEV. Assumptions of proposed optimization model are represented in Table 9.

The stochastic decentralized optimization approach of the MAS-based networked MEMGs is solved applying CPLEX solver under the GAMS 24.8.3 environment. It should be noted that all above hypotheses are not limited to the adjusted values and can vary based on any case study.

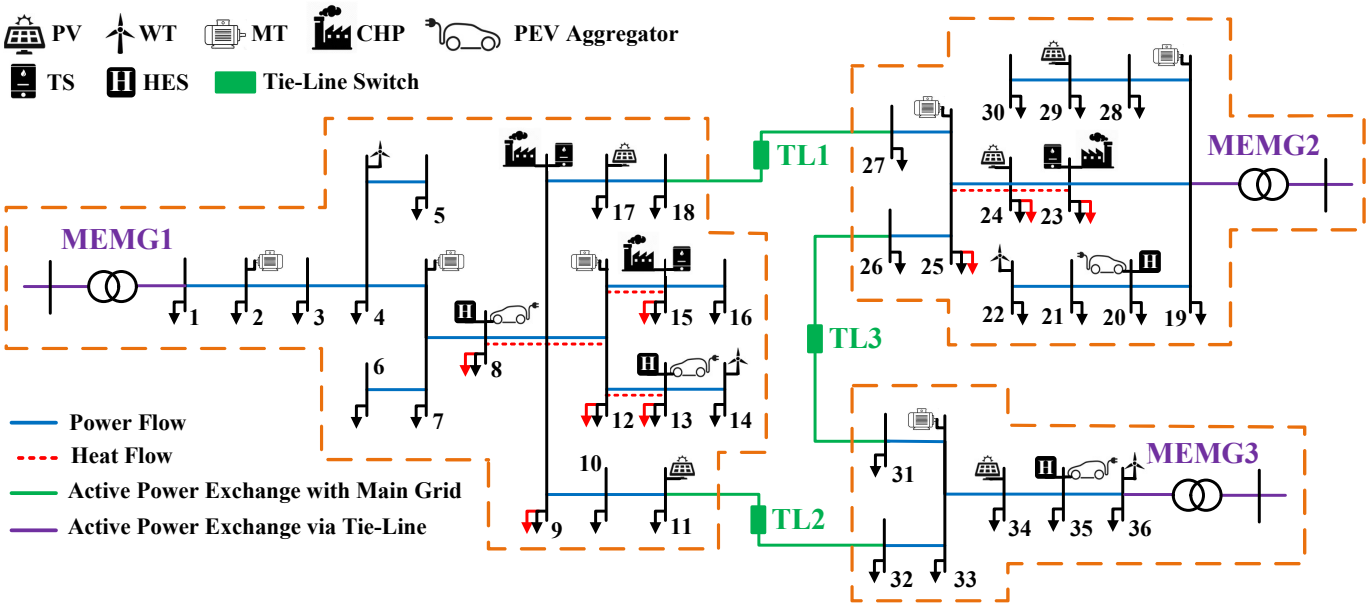

Figure 6: Test system with three MAS-based networked MEMGs

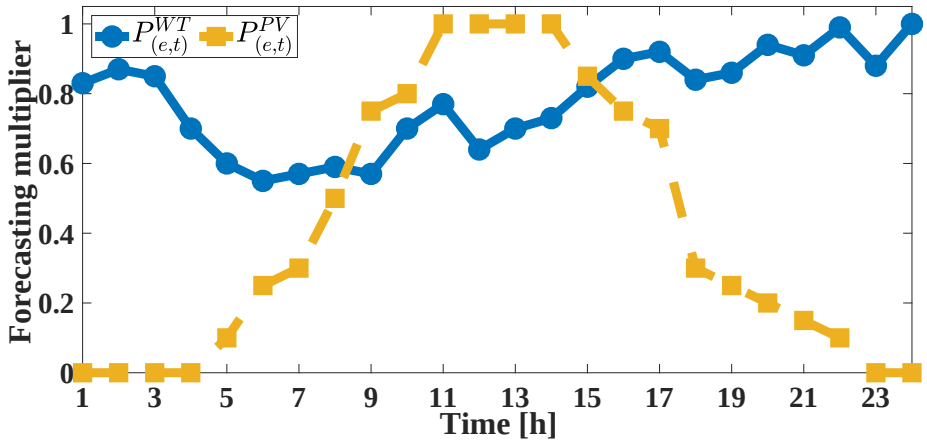

Figure 7: Hourly forecasted multipliers of renewable units

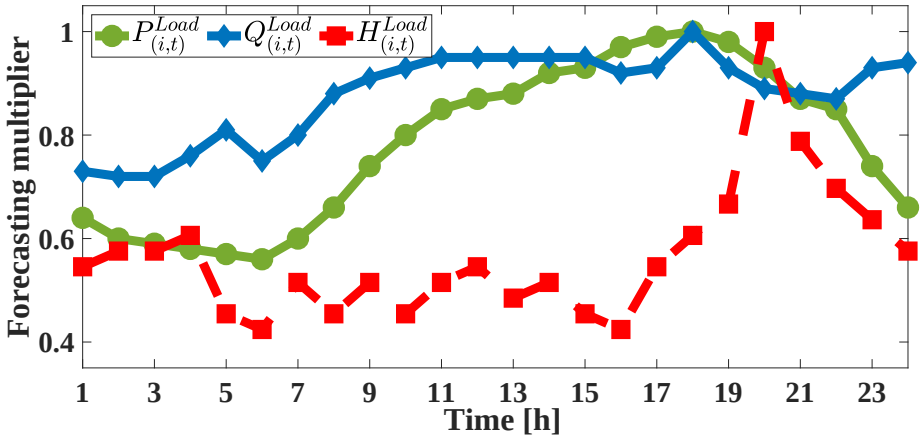

Figure 8: Hourly forecasted multipliers of active power, reactive power, and heat demands

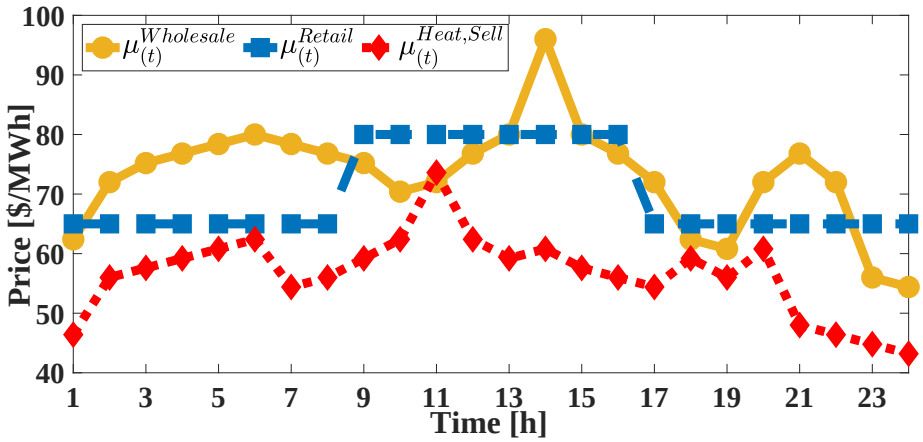

Figure 9: Hourly forecasted values of market prices

Table 2: Installed capacity and location of renewable units

MEMG #	**Location**	**Type**	**Capacity (MW)**
MEMG 1	Node 04	WT	0.5
	Node 11	PV	1.0
	Node 14	WT	2.5
	Node 17	PV	1.5
MEMG 2	Node 22	WT	2.0
	Node 24	PV	1.5
	Node 29	PV	2.5
MEMG 3	Node 34	PV	1.5
	Node 36	WT	1.0

Table 3: Location, technical, and economic data of MTs

MEMG #	**Location**	a ($/MW)	b ($/MW)	$\overline{P}^{MT}$ (MW)	$\overline{Q}^{MT}$ (MVAR)	$P^{MT,\,RU/RD}$ (MW)	$Q^{MT,\,RU/RD}$ (MVAR)
MEMG 1	Node 02	13.325	38.96	6	3	2.0	1.5
	Node 06	12.349	27.98	6	3	2.0	1.5
	Node 12	26.802	31.02	12	7	4.0	2.5
MEMG 2	Node 19	10.784	32.93	8	5	3.0	2.5
	Node 25	17.922	10.03	8	5	2.0	3.0
MEMG 3	Node 33	12.974	10.05	8	4	3.0	2.0

Table 4: Location and techno-economic data of CHP units

MEMG #	**Location**	$\phi^{CHP,\,1}$	$\phi^{CHP,\,2}$	$\phi^{CHP,\,3}$	$\psi^{CHP,\,1}$	$\psi^{CHP,\,2}$	$\psi^{CHP,\,3}$	$P^{CHP,\,RU}$	$P^{CHP,\,RD}$	UT^{CHP}	DT^{CHP}
MEMG 1	Node 09	0.035	36	12.5	0.027	1.6	0.011	4.94	4.94	3	3
	Node 15	0.044	14.5	26.5	0.03	4.2	0.031	2.14	2.14	3	3
MEMG 2	Node 23	0.038	25	17	0.019	3.7	0.039	3.02	3.02	3	3

Table 5: Feasible operation region data of CHP units (MW/MWth)

MEMG #	**Location**	PA^{CHP}	PB^{CHP}	PC^{CHP}	PD^{CHP}	PE^{CHP}	PF^{CHP}	HA^{CHP}	HB^{CHP}	HC^{CHP}	HD^{CHP}	HE^{CHP}	HF^{CHP}
MEMG 1	Node 09	4.94	4.3	1.62	1.98	0	0	0	3.6	2.09	0	0	0
	Node 15	2.14	2.14	1.87	0.68	0.75	0.75	0	0.55	2.64	1.27	0.27	0
MEMG 2	Node 23	3.02	3.02	2.64	0.96	1.06	1.06	0	0.78	3.73	1.8	0.38	0

Table 6: Characteristics of the TES (MWth)

MEMG #	**Location**	$\overline{B}^{ch}_{(c)}$	$\overline{B}^{dch}_{(c)}$	$\overline{B}_{(c)}$	$\underline{B}_{(c)}$
MEMG 1	Node 09	1.20	1.20	2.4	0
	Node 15	0.90	0.90	1.8	0
MEMG 2	Node 23	1.25	1.25	2.5	0

Table 7: Characteristics of the TES (MWth)

MEMG #	**Location**	$\overline{P}^{PEV}$	$\overline{E}^{PEV}$	$\underline{E}^{PEV}$	Number of Available PEVs
MEMG 1	Node 08	1.200	1.200	0.1200	4
	Node 13	1.125	1.125	0.1125	3
MEMG 2	Node 20	1.425	1.425	0.1425	4
MEMG 3	Node 35	0.750	0.750	0.0750	2

Table 8: Location and data of HESs (MW)

MEMG #	**Location**	$\overline{P}^{P2H}$	$\underline{P}^{P2H}$	$\overline{P}^{H2P}$	$\underline{P}^{H2P}$	$\overline{E}^{HES}$	$\underline{E}^{HES}$
MEMG 1	Node 08	0.20	0.04	0.20	0.04	0.60	0.12
	Node 13	0.30	0.06	0.30	0.06	0.90	0.18
MEMG 2	Node 20	0.30	0.06	0.30	0.06	1.00	0.20
MEMG 3	Node 35	0.15	0.03	0.15	0.03	0.50	0.10

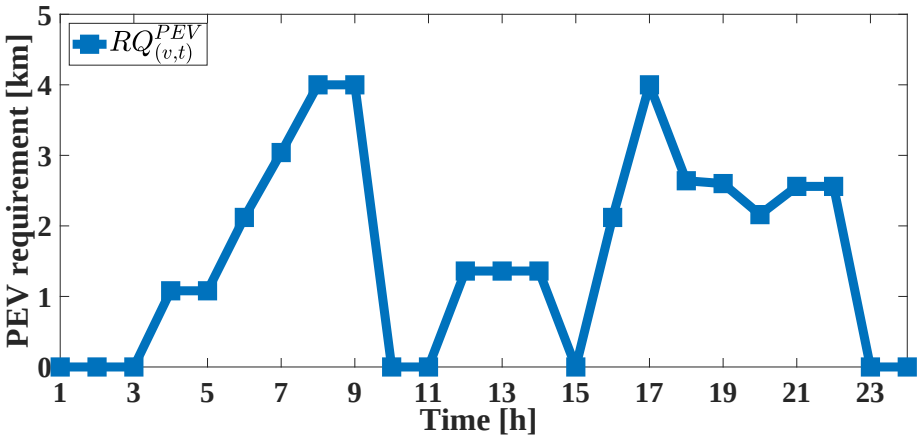

Figure 10: Forecasted values of driving requirement of each PEV

Table 9: Assumptions of proposed optimization model

Variable	Value	Variable	Value	Variable	Value
Power Base	10 MVA	$Y^{PEV}_{(v)}$	0.45 kWh/km	η^{TES}	0.99
$\overline{P}^{EX}_{(l)}$	10 MW	$\mu^{PEV}_{(t)}$	30 $/MWh	$\eta^{PEV,\,ch}$	0.95
$\overline{P}^{GR}_{(m)}$	10 MW	$\mu^{Hyd,\,Char}_{(t)}$	2 $/MWh	$\eta^{PEV,\,dch}$	0.95
$\underline{P}^{MT}_{(g)}$ / $\underline{Q}^{MT}_{(g)}$	0 MW/MVAR	$\mu^{Hyd,\,Sell}_{(t)}$	55 $/MWh	η^{P2H}	0.80
SU^{CHP}	0 $	λ^{loss}	0.60	λ^{loss}	0.60
SD^{CHP}	0 $	λ^{gain}	0.30	z	10

In this paper, three different scheduling case studies are defined for a more detailed analysis of the simulation results of the decentralized bi-level optimization approach as follows:

- **CS1**: Case without HESs with PEVs
- **CS2**: Case with HESs without PEVs
- **CS3**: Case with both HESs and PEVs

4.1. Numerical Results of MTs

Figures 11-13 illustrate the active power output of MTs in a 24-hour scheduling interval of the networked MEMGs in CS1-CS3, respectively. Comparing Figures 11 and 12 with Figure 13, it can be seen that the amount of total active power generation of MTs in off-peak hours in CS3 is increased very little compared to CS1, while is increased considerably compared to CS2. The total active power output of MTs in MEMG1 is approximately enhanced in CS3, while the total MT outputs in other MEMGs are almost unchanged compared to CS1 and CS2. Furthermore, the existing MTs in MEMG2 are off in all case studies. Accordingly, it can be mentioned that MEMGs need more energy to provide distance requirement of PEVs. Besides, the HES has little effect on the active power generation of MTs. Furthermore, the strategy of implementing power generation ramp-rates in the proposed approach deserves very well in such a manner that the ramp-rates of each MT between two scheduling hours are in their allowed value.

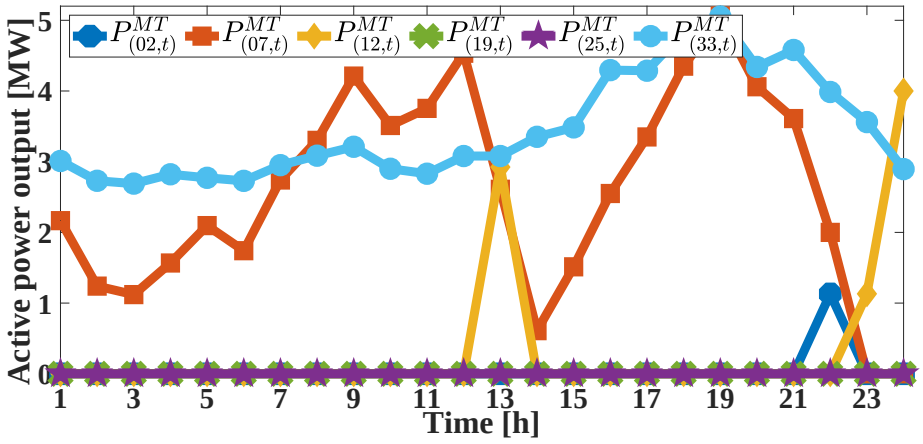

Figure 11: Active power output of MTs in CS1

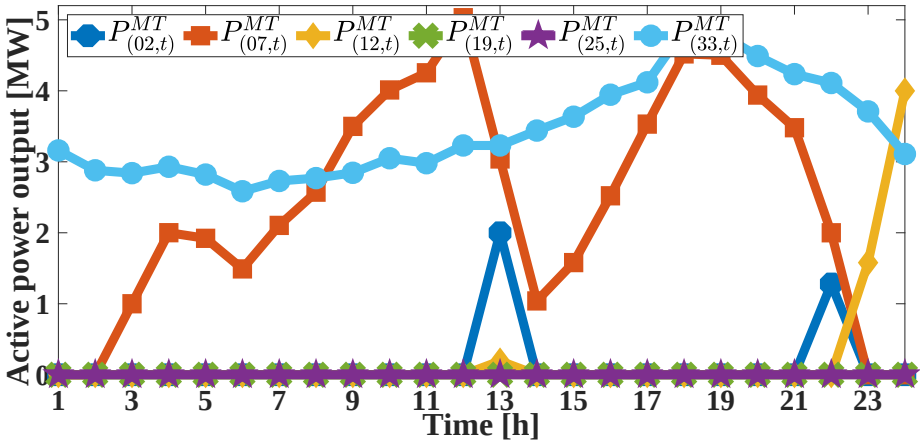

Figure 12: Active power output of MTs in CS2

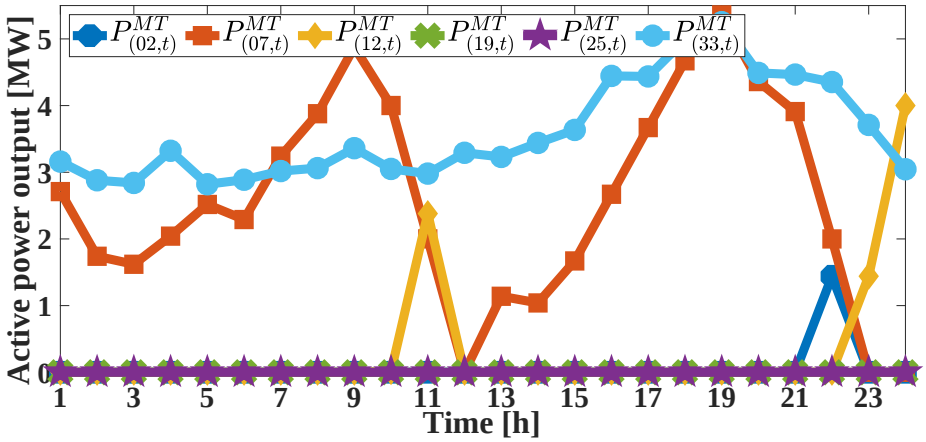

Figure 13: Active power output of MTs in CS3

4.2. Numerical Results of CHP Units and TESs

Figures 14-16 indicate the power and heat outputs of CHP units, and the value of heat storage of the TESs in CS1-CS3, respectively. As illustrated in Figure 6, the location of the CHP units and TESs are defined to be the same. Accordingly, the constraints of heat energy transmission are not taken into account. It can be seen from Figure 16 that the amount of power outputs of CHP units in CS3 almost remains unchanged compared to CS1, while reduced at hours 16 and 17 compared to CS2. Also, the total heat generation of CHP units and heat stored in TESs per hour is equal for all case studies. In general, the total amount of power/heat outputs of CHP units and total amount of heat storage in TESs are the same in all case studies. This means that the related optimization of the heating agent in the proposed MAS is independent of the hydrogen and transportation agents.

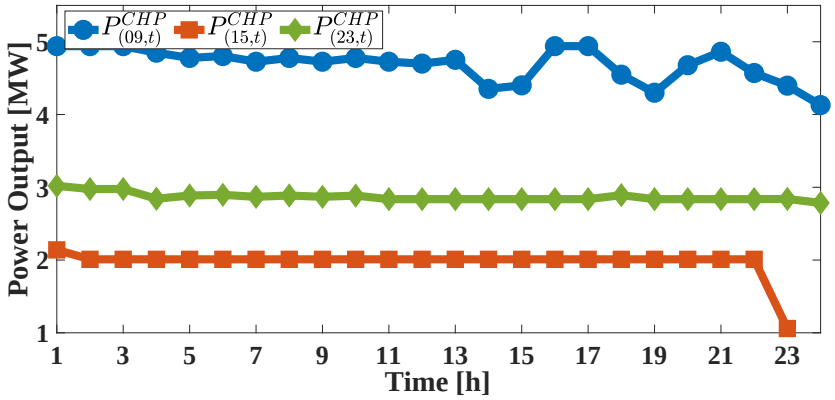

(a) Power outputs of CHP units

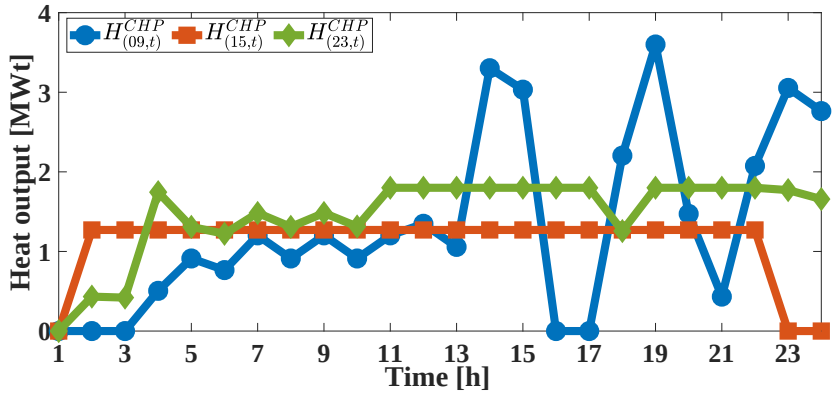

(b) Heat outputs of CHP units

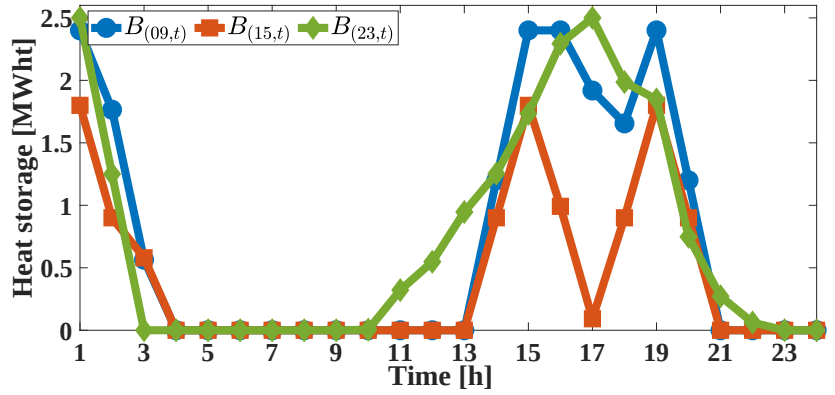

(c) Heat storage of TESs

Figure 14: Equipment output in CS1 (a) CHP power, (b) CHP heat, (c) TESs heat stored

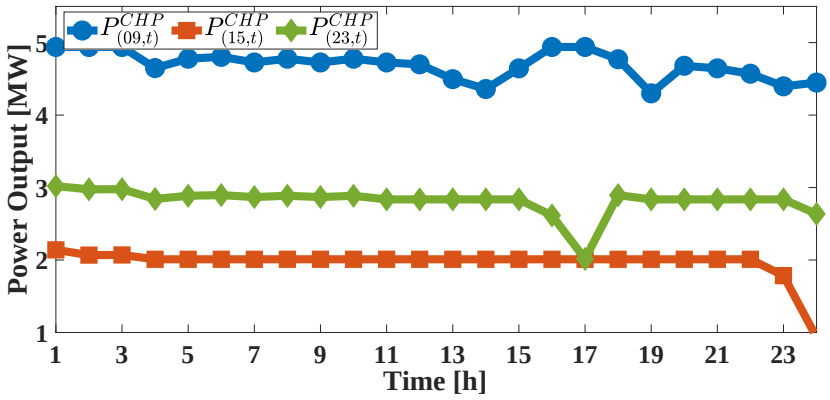

(a) Power outputs of CHP units

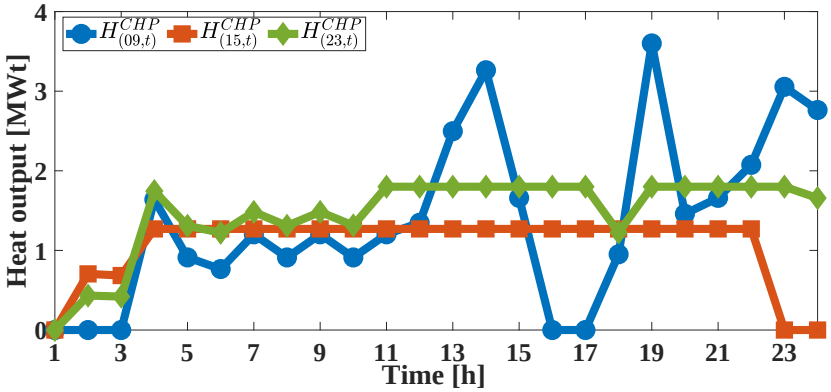

(b) Heat outputs of CHP units

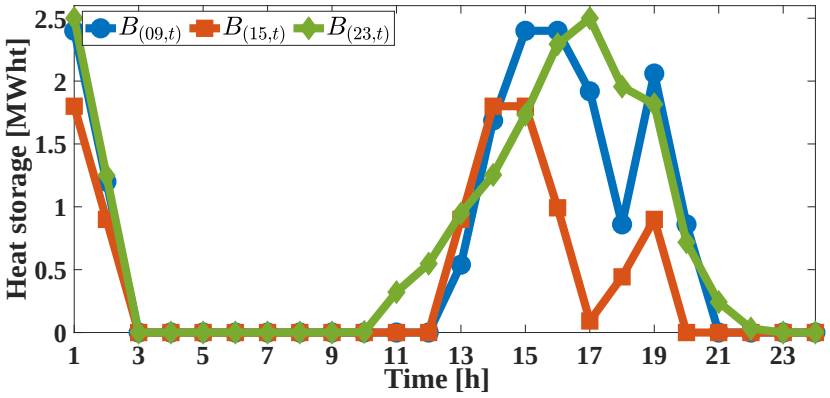

(c) Heat storage of TESs

Figure 15: Equipment output in CS2 (a) CHP power, (b) CHP heat, (c) TESs heat stored

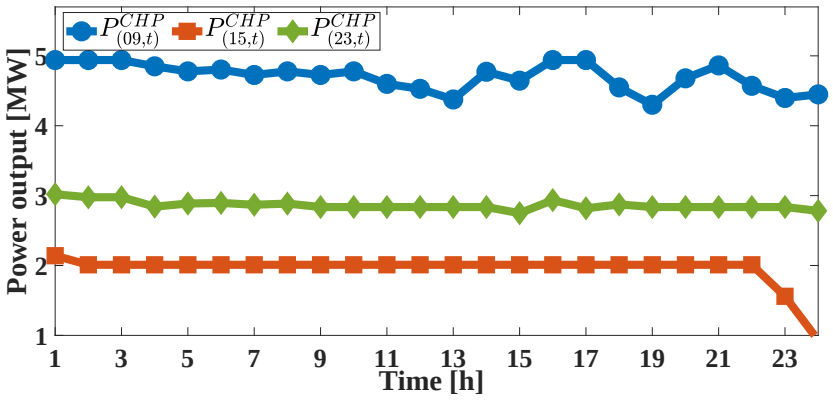

(a) Power outputs of CHP units

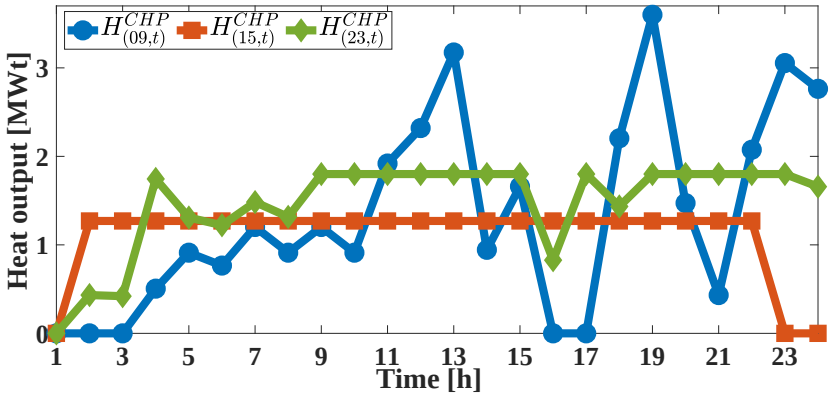

(b) Heat outputs of CHP units

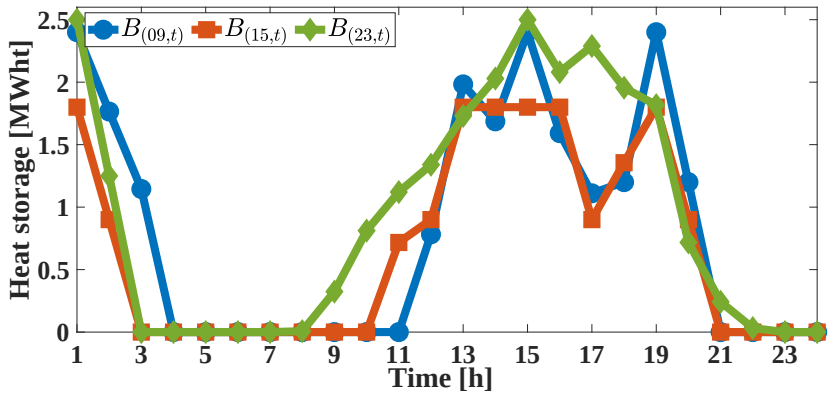

(c) Heat storage of TESs

Figure 16: Equipment output in CS3 (a) CHP power, (b) CHP heat, (c) TESs heat stored

4.3. Numerical Results of PEV Aggregators

The state of charge (SoC) of PEV aggregators in CS1 and CS3 are shown in Figures 17 and 18, respectively. It can be seen that amount of charging/discharging of PEVs is equal for both CS1 and CS3, however, the charging/discharging patterns are different. More charging/discharging is done in the CS1 because if there are HESs, less number of charge/discharge of PEVs is needed. The value of charging/discharging for both cases are equal to 6.26 MW, 5.51 MW, 7.37 MW, and 3.68 MW for PEV aggregators at nodes 8, 13, 20, and 35, respectively. This means that the transportation agent in the proposed MAS is independent of the hydrogen agent.

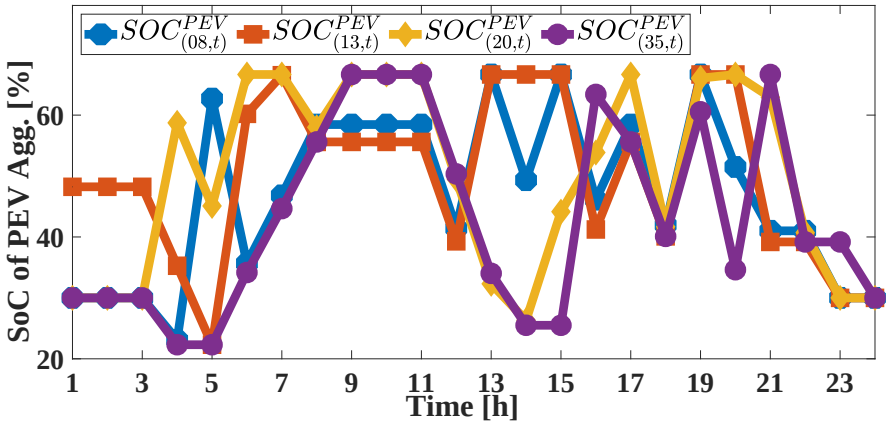

Figure 17: State of charge of PEV aggregators in CS1

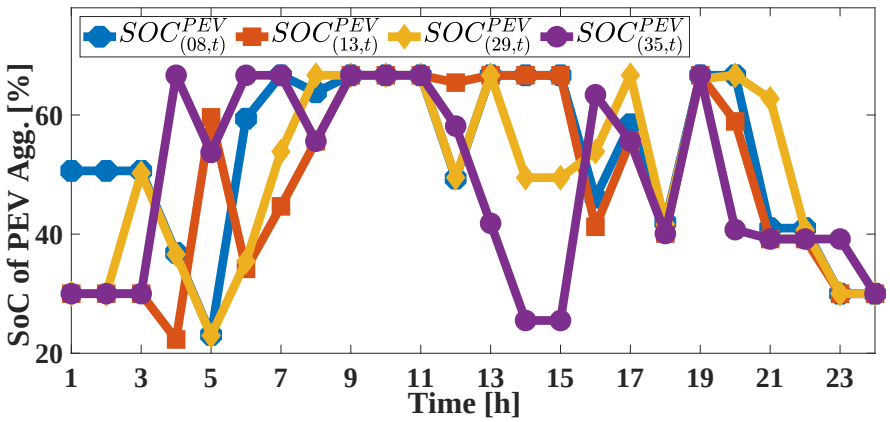

Figure 18: State of charge of PEV aggregators in CS3

4.4. Numerical Results of HESs

The SoC of the HES in CS2 and CS3 are presented in Figures 19 and 20, respectively. It can be seen that the amount of charging/discharging of HESs in CS2 is more than CS3. Thus, if there are PEVs, less amount of charge/discharge of HESs is required. it is worth noting that both P2H and the hydrogen delivery to the industry are affect the SoC of HESs. Also, based on the non-economic characteristic of the hydrogen energy returned to the network as the electrical form (H2P), the value of H2P in FCs is low for each HES in both CS2 and CS3.

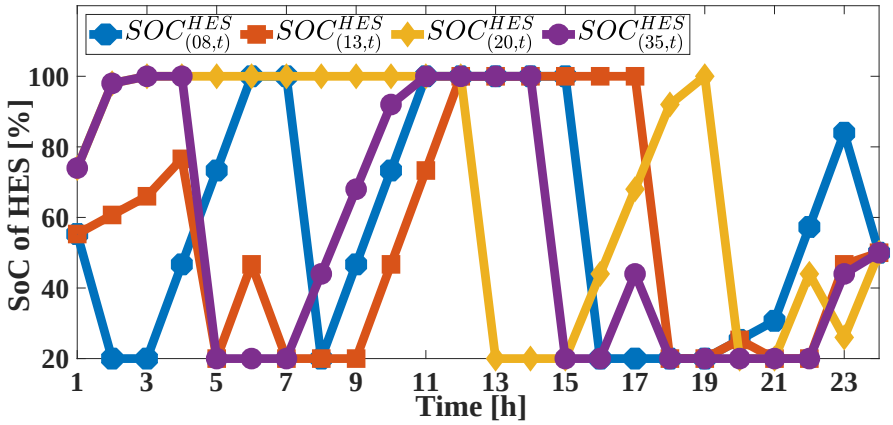

Figure 19: State of charge of HESs in CS2

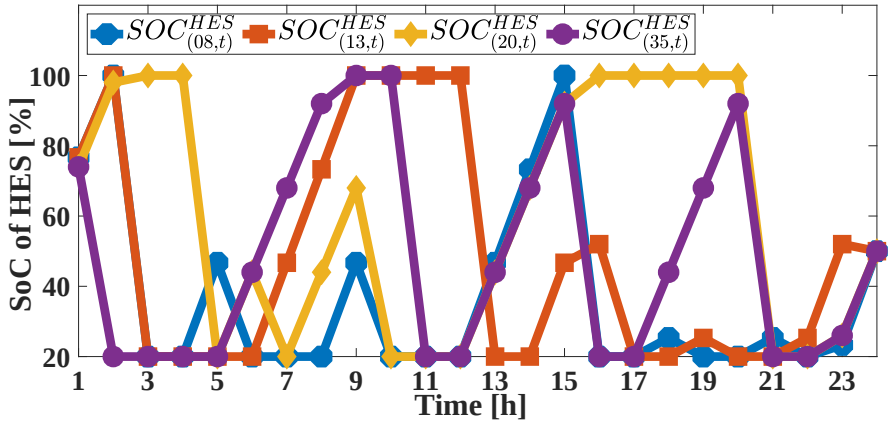

Figure 20: State of charge of HESs in CS3

The amount of hydrogen energy delivered to the industry in CS2 and CS3 are presented in Figures 21 and 22, respectively. The amounts of hydrogen energy delivered to the industry are obtained based on the interactions between the electricity and hydrogen agents in the proposed MAS framework. It can be mentioned that the amounts of hydrogen energy delivered to the industry in CS3 is 785 kW, equivalent to 20%, more than CS2 over a 24-hour scheduling. This means that PEVs have played an important role in increasing hydrogen energy delivery to the industry.

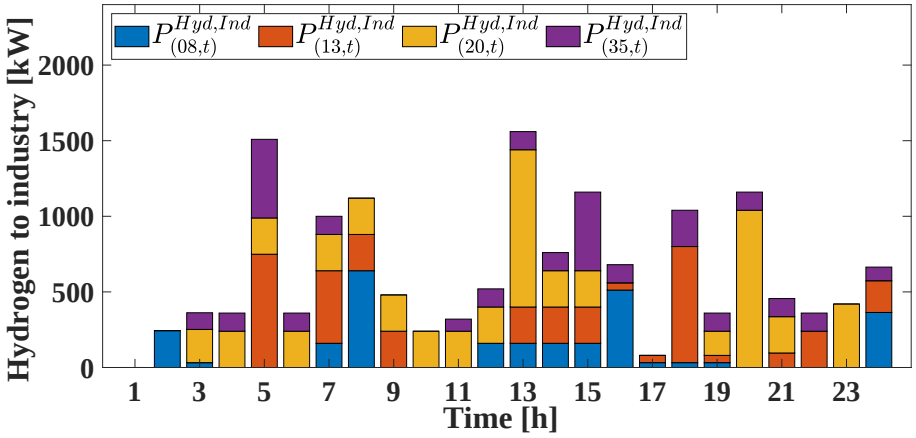

Figure 21: Amount of hydrogen energy delivered to the industry in CS2

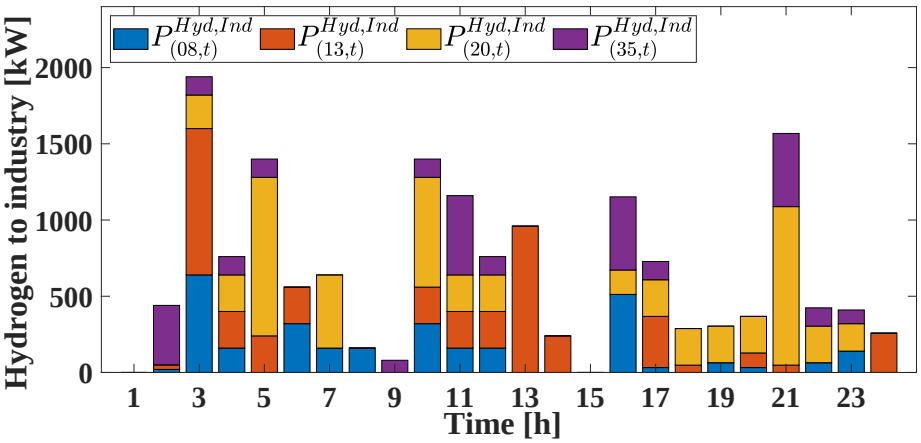

Figure 22: Amount of hydrogen energy delivered to the industry in CS3

4.5. Numerical Results of Power Exchanges

Figures 23-25 illustrate the active power exchanges among MEMGs and main grid in CS1-CS3, respectively. It should be mentioned that the positive values demonstrate that active power is exchanged from MEMG2 to MEMG1, MEMG3 to MEMG1, MEMG3 to MEMG2, and main grid to entire networked MEMGs. It can be seen from Figures 23-25 that the active power is exchanged only between MEMG1 to MEMG2, and from the main grid to MEMG1 in all case studies. This means that TL1 and TL3 switches are off during a 24-hour scheduling interval in all case studies. The total power exchange among the networked MEMGs in CS3 (Figure 25) is enhanced compared to CS1 (Figure 23). Also, the total power exchange in CS2 (Figure 24) is increased only at hours 1 and 2, while reduced at other hours compared to CS3. This means that utilizing multi-energy storage systems have an important role in increasing power exchanges among the networked MEMGs.

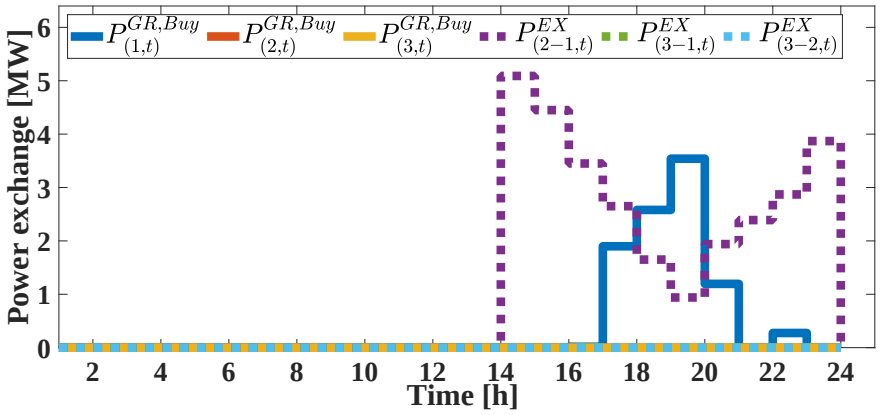

Figure 23: Active power exchanges between MEMGs and main grid in CS1

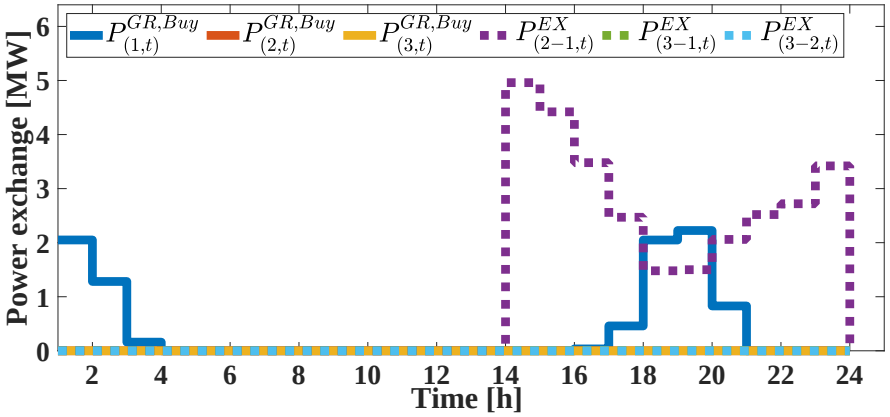

Figure 24: Active power exchanges between MEMGs and main grid in CS2

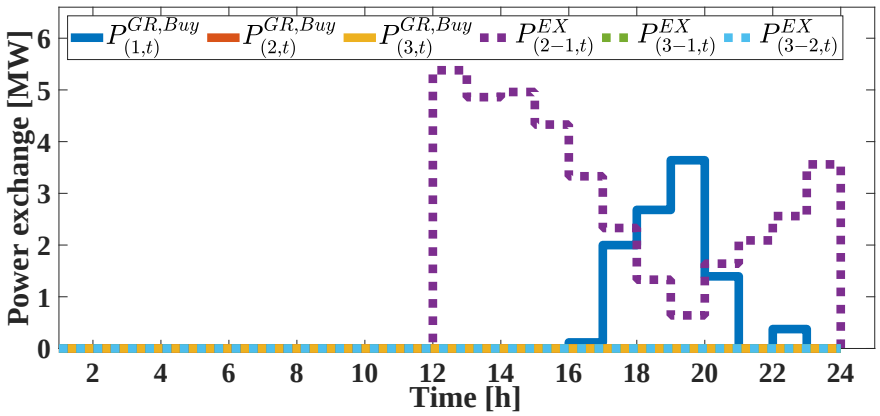

Figure 25: Active power exchanges between MEMGs and main grid in CS3

To investigate in more detail how the active power exchanges are converged, the values of the power exchanges among the MEMGs in the iterations at hour 18 as an example are illustrated for CS1-CS3 in Figures 26-28, respectively. It can be realized from comparison of Figures 26-28 that all MEMGs want to sell active power to other MEMGs at the early iterations. After seven iterations, the negotiations between all MEMGs are achieved in all case studies.

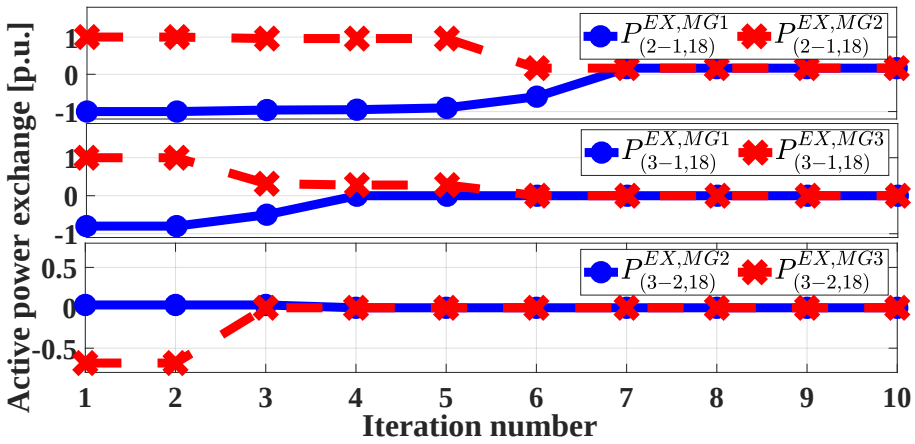

Figure 26: Active power exchange convergence between MEMGs at hour 18 in CS1

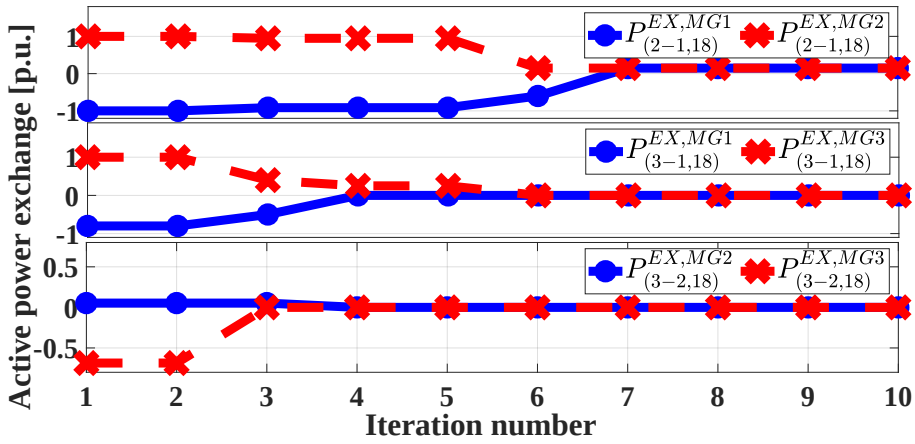

Figure 27: Active power exchange convergence between MEMGs at hour 18 in CS2

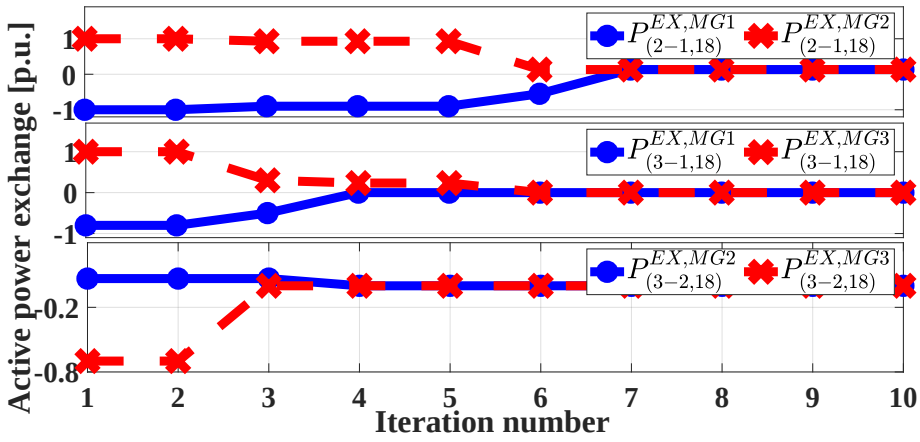

Figure 28: Active power exchange convergence between MEMGs at hour 18 in CS3

4.6. Numerical Results of Voltage Magnitude

The voltage of the nodes on a 24-hour scheduling of MEMGs in CS1-CS3 are shown in Figures 29-31, respectively. It is clear that all voltage values are in their allowed deviation limit for all case studies. It can be seen from Figures 29-31 that the voltage regulation in CS2 and CS3 are almost the same and are generally more favorable than values in CS1. This means that implementing HESs in the MEMG model has played an effective role in regulating the voltage level, while the employment of PEVs has been almost unaffected.

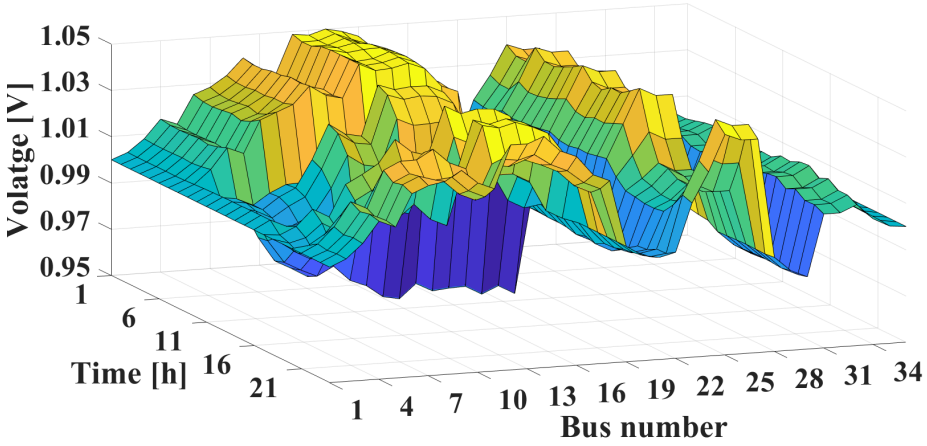

Figure 29: Voltage magnitude of nodes in CS1

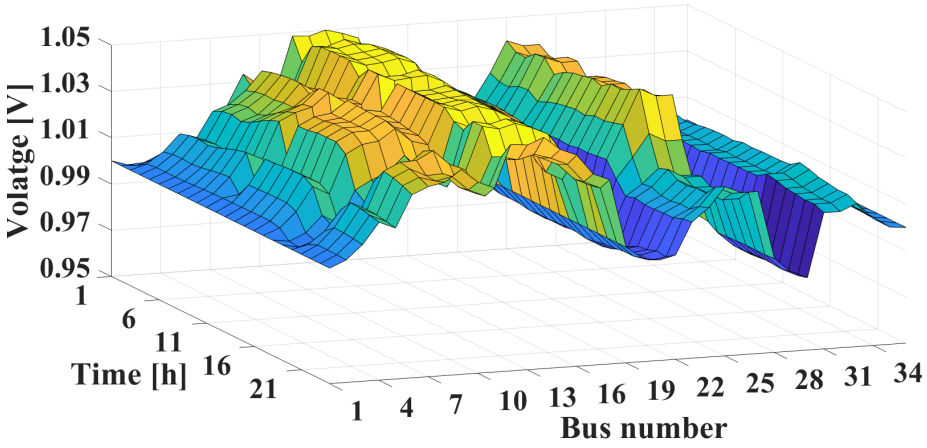

Figure 30: Voltage magnitude of nodes in CS2

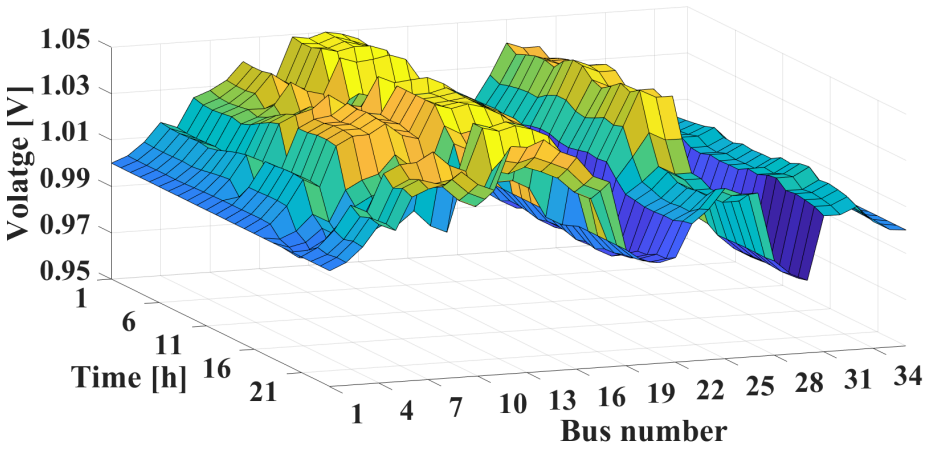

Figure 31: Voltage magnitude of nodes in CS3

4.7. Numerical Results of Penalty Prices

The hourly calculated penalty prices to achieve an agreement among the networked MEMGs in all case studies are illustrated in Figure 32. As it is obvious from Figure 32, the penalty price in CS1 and CS2 at hours 12 and 13 is higher than CS3. Also, the calculated penalty prices are reduced at peak hours in all case studies. This means that there is less disparity between MEMGs to exchange power during peak hours when the HESs are considered in the model, while the employment of PEVs has almost no effect on the penalty prices.

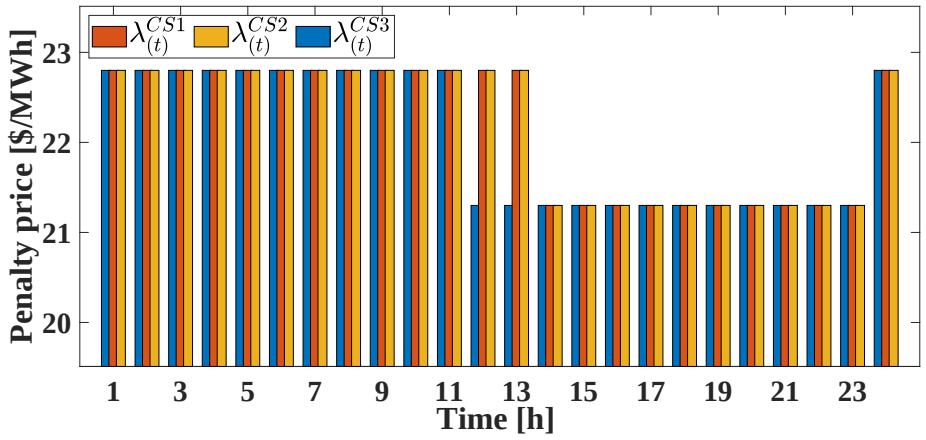

Figure 32: Hourly calculated penalty price in all case studies

4.8. Numerical Results of Operation Costs and Revenues

According to the objective function formulated by Eq. (13), the operational expenses, revenues, and total profits of each MEMGs and the entire networked system are illustrated in details in Tables 10-12 at a 24-hour scheduling interval for CS1-CS3, respectively. Besides, the total profit of each MEMGs and the entire networked system for the deterministic optimization approach is also presented for all case studies as a detailed comparison of the proposed stochastic optimization strategy. As it is clear from Tables 10-12, the total profit of each MEMGs and the entire networked system for the stochastic optimization strategy is higher than the deterministic approach in all case studies. Furthermore, the total profit of the networked MEMGs for the stochastic optimization strategy in CS3 is $630.5 higher than CS1 and $688.268 higher than CS2. It can be also seen from Tables 10-12 that the revenues of selling electricity and heat to consumers, and driving requirements of PEVs in all case studies remain unchanged.

Table 10: Detailed cost and revenue results in CS1

Optimization Approach	Detail ($)	MEMG1	MEMG2	MEMG3	Networked MEMGs
Stochastic	$\mathscr{R}^{\text{Load}}$	24704.064	16469.376	8234.688	49408.128
	$\mathscr{R}^{\text{CHP}}$	2286.218	1371.598	0	3657.816
	$\mathscr{R}^{\text{PEV}}$	817.182	510.739	255.37	1583.291
	$\mathscr{C}^{\text{PEV}}$	342.772	214.538	106.819	664.129
	$\mathscr{C}^{\text{CHP}}$	5820.57	2259.072	0	8079.642
	$\mathscr{C}^{\text{EX}}$	982.81	-982.81	0	0
	$\mathscr{C}^{\text{MT}}$	1740.42	0	1312.346	3052.766
	$\mathscr{C}^{\text{GR}}$	620.098	0	0	620.098
	$\mathscr{R}^{\text{GR}}$	0	0	0	0
	Total Profit	18300.795	16860.913	7070.893	42232.601
Deterministic	Total Profit	18191.645	15054.386	7049.7437	40295.775

Table 11: Detailed cost and revenue results in CS2

Optimization Approach	Detail ($)	MEMG1	MEMG2	MEMG3	Networked MEMGs
Stochastic	$\mathscr{R}^{\text{Load}}$	24704.064	16469.376	8234.688	49408.128
	$\mathscr{R}^{\text{CHP}}$	2286.218	1371.598	0	3657.816
	$\mathscr{R}^{\text{HES}}$	328.75	288	144	760.75
	$\mathscr{C}^{\text{HES}}$	16.44	14.4	7.2	38.04
	$\mathscr{C}^{\text{CHP}}$	5836.754	2229.265	0	8066.019
	$\mathscr{C}^{\text{EX}}$	973.753	-973.753	0	0
	$\mathscr{C}^{\text{MT}}$	1645.675	0	1311.555	2957.23
	$\mathscr{C}^{\text{GR}}$	590.672	0	0	590.672
	$\mathscr{R}^{\text{GR}}$	0	0	0	0
	Total Profit	18255.737	16859.063	7060.033	42174.833
Deterministic	Total Profit	18146.855	15052.734	7038.916	40240.656

Table 12: Detailed cost and revenue results in CS3

Optimization Approach	Detail ($)	MEMG1	MEMG2	MEMG3	Networked MEMGs
Stochastic	$\mathscr{R}^{\text{Load}}$	24704.064	16469.376	8234.688	49408.128
	$\mathscr{R}^{\text{CHP}}$	2286.218	1371.598	0	3657.816
	$\mathscr{R}^{\text{PEV}}$	817.182	510.739	255.37	1583.291
	$\mathscr{R}^{\text{HES}}$	378	288	144	810
	$\mathscr{C}^{\text{PEV}}$	342.744	214.538V	106.847	664.129
	$\mathscr{C}^{\text{HES}}$	18.4	14.4	7.2	40
	$\mathscr{C}^{\text{CHP}}$	5841.616	2256.364	0	8097.98
	$\mathscr{C}^{\text{EX}}$	1241.426	-1241.426	0	0
	$\mathscr{C}^{\text{MT}}$	1766.063	0	1359.066	3125.129
	$\mathscr{C}^{\text{GR}}$	668.898	0	0	668.898
	$\mathscr{R}^{\text{GR}}$	0	0	0	0
	Total Profit	18300.795	16860.913	7070.893	42232.601
Deterministic	Total Profit	18191.645	15054.386	7049.743	40295.775

4.9. Numerical Results of Diverse Network Topologies

For the sake of a detailed analysis, the results of the proposed approach as the base value, is compared with diverse switch status forms of the network topology for CS1-CS3 in Tables 13-15, respectively. It can be seen that the total profit of networked MEMGs in all switch status forms are equal to the base values for all case studies. This means that the networked MEMGs using the proposed approach are converged in the same profit, but with a difference that the profit of each MEMG has slightly changed in its independent operation. As a result, the proposed approach has the necessary merit to operate MEMGs in diverse topologies.

Table 13: Total profit changes with diverse switch statuses compared to the proposed topology in CS1

Switch Status			**Total Profit Changes (%)**			
TL12	TL13	TL23	MEMG 1	MEMG 2	MEMG 3	Networked MEMGs
✔	✔	✔	Base Value I	Base Value II	Base Value III	Total Value
✔	✔	✖	No Change	No Change	No Change	No Change
✔	✖	✔	No Change	No Change	No Change	No Change
✖	✔	✔	-0.21	-0.76	+2.35	No Change
✔	✖	✖	No Change	No Change	No Change	No Change
✖	✔	✖	-0.67	+0.66	+0.16	No Change
✖	✖	✔	-0.61	+0.22	+1.05	No Change
✖	✖	✖	-0.61	+0.66	No Change	No Change

Table 14: Total profit changes with diverse switch statuses compared to the proposed topology in CS2

Switch Status			**Total Profit Changes (%)**			
TL12	TL13	TL23	MEMG 1	MEMG 2	MEMG 3	Networked MEMGs
✔	✔	✔	Base Value I	Base Value II	Base Value III	Total Value
✔	✔	✖	No Change	No Change	No Change	No Change
✔	✖	✔	No Change	No Change	No Change	No Change
✖	✔	✔	-0.43	-1.68	+5.12	No Change
✔	✖	✖	No Change	No Change	No Change	No Change
✖	✔	✖	-1.24	+1.05	+0.69	No Change
✖	✖	✔	-0.97	+0.38	+1.60	No Change
✖	✖	✖	-0.97	+1.05	No Change	No Change

Table 15: Total profit changes with diverse switch statuses compared to the proposed topology in CS3

Switch Status			**Total Profit Changes (%)**			
TL12	TL13	TL23	MEMG 1	MEMG 2	MEMG 3	Networked MEMGs
✔	✔	✔	Base Value I	Base Value II	Base Value III	Total Value
✔	✔	✖	No Change	No Change	No Change	No Change
✔	✖	✔	No Change	No Change	No Change	No Change
✖	✔	✔	-0.59	- 2.39	+7.32	No Change
✔	✖	✖	No Change	No Change	No Change	No Change
✖	✔	✖	-1.64	+1.52	+0.51	No Change
✖	✖	✔	-1.44	+0.53	+2.29	No Change
✖	✖	✖	-1.44	+1.52	No Change	No Change

5. Conclusion

In this paper, a novel structure for MAS-based networked MEMGs (including power, heat, and hydrogen energy carriers) was proposed considering CHP units, TES, PEVs aggregators, and HESs to meet the diverse energy consumers. Also, a novel flexible decentralized bi-level stochastic optimization approach based on the progressive hedging algorithm was introduced for the proposed structure considering power, heat, and hydrogen energy supplier and consumers. The P2H and H2P facilities were also utilized along with the HES to increase the overall profit and efficiency of the multi-agent networked multi-energy microgrids and consider the hydrogen-based consumers and industry. The LHS method was selected to handle the related uncertainty of the renewable units, active/reactive power and heat consumptions, and distance requirements of PEVs. Also, a novel penalty function was developed for the convergence of the agreed energy exchanges among the multi-agent networked multi-energy microgrids taking into account the self-sufficiency of each agent. The derived model was simulated over a multi-agent system with three microgrids maximizing the total profit of each microgrid over a 24-hour time horizon operation.

One of the main advantages of the proposed framework is that connecting a new agent with specific attributes to the proposed networked MEMGs is feasible due to

the configurability feature of the proposed optimization algorithm. In addition, the agent's objectives, tasks and accessibility to other agent's data can be modified during the MAS-based network operation. Besides, the scalability feature allows the integration of new loads, generations and agents without affecting the simplicity and computational process of the proposed modified progressive hedging algorithm.

According to the main achievements of the result section with three diverse case studies, it can be concluded that:

- Each agent in the proposed structure of MEMGs were self-sufficient in the scheduling optimization problem in such a way that electricity and heating agents were self-determining of the transportation and hydrogen-based agents' performance in all case studies;
- Utilizing the conversion facilities plays a crucial role in enhancing total profit of MEMGs and improving the reliability performance of MAS-based structure;
- A reliable MAS-based framework can be achieved through a little data exchange, which protect the data privacy of agents belonging to different stakeholders.;
- The optimal scheduling of the networked MEMGs using the proposed optimization approach were converged in the same profit for the diverse network topologies considering diverse tie-line switch forms, but with this difference that the profit of each MEMGs had slightly varied in its self-scheduling optimization;
- Finally, the proposed bi-level optimization approach, by converging through seven iterations, showed an effective performance as a promising solution to a decentralized framework. Also, the proposed optimization approach could contribute to more efficient market operation for multi-stakeholder MEMGs.

Based on the proposed MAS-based framework of the networked MEMGs, occurrence of emergency situation and general strategies for enhancing the flexibility of the DSs in response to the proposed local optimization in each MEMG can be studied in future researches. Furthermore, the self-healing concepts can also be proposed to investigate the interconnection and flexibility enhancement capabilities of the networked MEMGs toward an intelligent emergency operation.

6. Acknowledgments

The Authors acknowledge the support provided by King Abdullah City for Atomic and Renewable Energy (K.A.CARE) under K.A.CARE-King Abdulaziz University Collaboration Program. The authors are also thankful to Deanship of Scientific Research, King Abdulaziz University for providing financial support vide grant number (RG-11-135-42).

References

[1] H. Zuo, B. Zhang, Z. Huang, K. Wei, H. Zhu, J. Tan, Effect analysis on soc values of the power lithium manganate battery during discharging process and its intelligent estimation, Energy 238, Part B (2022) 121854.

[2] X. Zhao, J. E, G. Wu, Y. Deng, D. Han, B. Zhang, Z. Zhang, A review of studies using graphenes in energy conversion, energy storage and heat transfer development, Energy Conversion and Management 184 (2019) 581–599.

[3] M. A. Mirzaei, A. Sadeghi-Yazdankhah, M. M. Behnam Mohammadi-Ivatloo, M. Shafie-khah, J. P. Catalão, Integration of emerging resources in igdt-based robust scheduling of combined power and natural gas systems considering flexible ramping products, Energy 189 (2019) 116195.

[4] H. Karimi, S. Jadid, Optimal energy management for multi-microgrid considering demand response programs: A stochastic multi-objective framework, Energy 195 (2020) 116992.

[5] E. Bullich-Massagué, F. Díaz-González, M. Aragüés-Peñalba, F. Girbau-Llistuella, P. Olivella-Rosell, A. Sumper, Microgrid clustering architectures, Applied Energy 212 (2018) 340–361.

[6] D. Sadeghi, A. H. Naghshbandy, S. Bahramara, Optimal sizing of hybrid renewable energy systems in presence of electric vehicles using multi-objective particle swarm optimization, Energy 209 (2020) 118471.

[7] S. E. Ahmadi, N. Rezaei, Distribution network emergency operation in the light of flexibility, in: Flexibility in Electric Power Distribution Networks, CRC Press, 2021, pp. 147–174.

[8] S. E. Ahmadi, N. Rezaei, H. Khayyam, Energy management system of networked microgrids through optimal reliability-oriented day-ahead self-healing scheduling, Sustainable Energy, Grids and Networks 23 (2020) 100387.

[9] S. E. Ahmadi, N. Rezaei, An igdt-based robust optimization model for optimal operational planning of cooperative microgrid clusters: A normal boundary intersection multi-objective approach, International Journal of Electrical Power Energy Systems 127 (2021) 106634.

[10] M. W. Khan, J. Wang, L. Xiong, Optimal energy scheduling strategy for multi-energy generation grid using multi-agent systems, International Journal of Electrical Power Energy Systems 124 (2021) 106400.

[11] N. Nasiri, A. Sadeghi Yazdankhah, M. A. Mirzaei, A. Loni, B. Mohammadi-Ivatloo, K. Zare, M. Marzband, A bi-level market-clearing for coordinated regional-local multi-carrier systems in presence of energy storage technologies, Sustainable Cities and Society 63 (2020) 102439.

[12] X. Ding, Q. Guo, T. Qiannan, K. Jermsittiparsert, Economic and environmental assessment of multi-energy microgrids under a hybrid optimization technique, Sustainable Cities and Society 65 (2021) 102630.

[13] S. Sharma, A. Verma, Y. Xu, B. K. Panigrahi, Robustly coordinated bi-level energy management of a multi-energy building under multiple uncertainties, IEEE Transactions on Sustainable Energy 12 (1) (2021) 3–13.

[14] Y. Teng, P. Sun, Q. Hui, Y. Li, Z. Chen, A model of electro-thermal hybrid energy storage system for autonomous control capability enhancement of multi-energy microgrid, CSEE Journal of Power and Energy Systems 5 (4) (2019) 489–497.

[15] N. Nasiri, A. Sadeghi Yazdankhah, M. A. Mirzaei, A. Loni, B. Mohammadi-Ivatloo, K. Zare, M. Marzband, Interval optimization-based scheduling of interlinked power, gas, heat, and hydrogen systems, IET Renewable Power Generation 15 (6) (2021) 1214–1226.

[16] A. Anvari-Moghaddam, A. Rahimi-Kian, M. S. Mirian, J. M. Guerrero, A multi-agent based energy management solution for integrated buildings and microgrid system, Applied Energy 203 (2017) 41–56.

[17] A. M. Alishavandi, S. M. Moghaddas-Tafreshi, Interactive decentralized operation with effective presence of renewable energies using multi-agent systems, International Journal of Electrical Power & Energy Systems 112 (2019) 36–48.

[18] B. Hong, W. Zhang, Y. Zhou, J. Chen, Y. Xiang, Y. Mu, Energy-internet-oriented microgrid energy management system architecture and its application in china, Applied Energy 228 (2018) 2153–2164.

[19] S. M. Nosratabadi, R. Hemmati, M. Jahandide, Eco-environmental planning of various energy storages within multi-energy microgrid by stochastic price-based programming inclusive of demand response paradigm, Journal of Energy Storage 36 (2021) 102418.

[20] J. Liu, X. Cao, Z. Xu, X. Guan, X. Dong, C. Wang, Resilient operation of multi-energy industrial park based on integrated hydrogen-electricity-heat microgrids, International Journal of Hydrogen Energy (2021).

[21] A. Ghanbari, H. Karimi, S. Jadid, Optimal planning and operation of multi-carrier networked microgrids considering multi-energy hubs in distribution networks, Energy 204 (2020) 117936.

[22] Y. Li, F. Zhang, Y. Li, Y. Wang, An improved two-stage robust optimization model for cchp-p2g microgrid system considering multi-energy operation under wind power outputs uncertainties, Energy 223 (2021) 120048.

[23] A. Mansour-Saatloo, M. A. Mirzaei, B. Mohammadi-Ivatloo, K. Zare, A risk-averse hybrid approach for optimal participation of power-to-hydrogen

technology-based multi-energy microgrid in multi-energy markets, Sustainable Cities and Society 63 (2020) 102421.

[24] M. Z. Oskouei, M. A. Mirzaei, B. Mohammadi-Ivatloo, M. Shafiee, M. Marzband, A. Anvari-Moghaddam, A hybrid robust-stochastic approach to evaluate the profit of a multi-energy retailer in tri-layer energy markets, Energy 214 (2021) 118948.

[25] N. Nasiri, S. Zeynali, S. N. Ravadanegh, M. Marzband, A hybrid robust-stochastic approach for strategic scheduling of a multi-energy system as a price-maker player in day-ahead wholesale market, Energy 235 (2021) 121398.

[26] S. E. Ahmadi, N. Rezaei, A new isolated renewable based multi microgrid optimal energy management system considering uncertainty and demand response, International Journal of Electrical Power & Energy Systems 118 (2020) 105760.

[27] A. Dini, S. Pirouzi, M. Norouzi, M. Lehtonen, Grid-connected energy hubs in the coordinated multi-energy management based on day-ahead market framework, Energy 188 (2019) 116055.

[28] N. Nikmehr, Distributed robust operational optimization of networked microgrids embedded interconnected energy hubs, Energy 199 (2020) 117440.

[29] H. Qiu, F. You, Decentralized-distributed robust electric power scheduling for multi-microgrid systems, Applied Energy 269 (2020) 115146.

[30] X. Zhou, Q. Ai, M. Yousif, Two kinds of decentralized robust economic dispatch framework combined distribution network and multi-microgrids, Applied Energy 253 (2019) 113588.

[31] Y. Kou, Z. Bie, G. Li, F. Liu, J. Jiang, Reliability evaluation of multi-agent integrated energy systems with fully distributed communication, Energy 224 (2021) 120123.

[32] E. Samadi, A. Badri, R. Ebrahimpour, Decentralized multi-agent based energy management of microgrid using reinforcement learning, International Journal of Electrical Power & Energy Systems 122 (2020) 106211.

[33] W. Jiang, K. Yang, J. Yang, R. Mao, N. Xue, Z. Zhuo, A multiagent-based hierarchical energy management strategy for maximization of renewable energy consumption in interconnected multi-microgrids, IEEE Access 7 (2019) 169931–169945.

[34] X. Wang, C. Wang, T. Xu, L. Guo, P. Li, L. Yu, H. Meng, Optimal voltage regulation for distribution networks with multi-microgrids, Applied Energy 210 (2018) 1027–1036.

[35] Q. Li, M. Gao, H. Lin, Z. Chen, M. Chen, Mas-based distributed control method for multi-microgrids with high-penetration renewable energy, Energy 171 (2019) 284–295.

[36] K. Yang, C. Li, X. Jing, Z. Zhu, Y. Wang, H. Ma, Y. Zhang, Energy dispatch optimization of islanded multi-microgrids based on symbiotic organisms search and improved multi-agent consensus algorithm, Energy 239, Part C (2022) 122105.

[37] M. A. Mohamed, T. Jin, W. Su, Multi-agent energy management of smart islands using primal-dual method of multipliers, Energy 208 (2020) 118306.

[38] H. Gao, J. Liu, L. Wang, Z. Wei, Decentralized energy management for networked microgrids in future distribution systems, IEEE Transactions on Power Systems 33 (4) (2018) 3599–3610.

[39] H. Gao, S. Xu, Y. Liu, L. Wang, Y. Xiang, J. Liu, Decentralized optimal operation model for cooperative microgrids considering renewable energy uncertainties, Applied Energy 262 (2020) 114579.

[40] P. Mathew, S. Madichetty, S. Mishra, A multilevel distributed hybrid control scheme for islanded dc microgrids, IEEE Systems Journal 13 (4) (2019) 4200–4207.

[41] M. Kabli, M. A. Quddus, S. G. Nurre, M. Marufuzzaman, J. M. Usher, A stochastic programming approach for electric vehicle charging station expansion plans, International Journal of Production Economics 220 (2020) 107461.

[42] M. Mazidi, A. Zakariazadeh, S. Jadid, P. Siano, Integrated scheduling of renewable generation and demand response programs in a microgrid, Energy Conversion and Management 86 (2014) 1118–1127.

[43] D. Donovan, K. Burrage, P. Burrage, T. McCourt, B. Thompson, E. Yazici, Estimates of the coverage of parameter space by latin hypercube and orthogonal array-based sampling, Applied Mathematical Modelling 57 (2018) 553–564.

[44] R. Sheikholeslami, S. Razavi, Progressive latin hypercube sampling: An efficient approach for robust sampling-based analysis of environmental models, Environmental Modelling Software 93 (2017) 109–126.

[45] W. Römisch, Scenario reduction techniques in stochastic programming, in: O. Watanabe, T. Zeugmann (Eds.), Stochastic Algorithms: Foundations and Applications, Springer, Berlin, Heidelberg, 2009, pp. 1–14.

[46] L. Meeus, L. Vandezande, S. Cole, R. Belmans, Market coupling and the importance of price coordination between power exchanges, Energy 34 (3) (2009) 228–234.

[47] M. Baran, F. Wu, Network reconfiguration in distribution systems for loss reduction and load balancing, IEEE Transactions on Power Delivery 4 (2) (1989) 1401–1407.

[48] M. Nazari-Heris, B. Mohammadi-Ivatloo, G. B. Gharehpetian, M. Shahidehpour, Robust short-term scheduling of integrated heat and power microgrids, IEEE Systems Journal 13 (3) (2019) 3295–3303.

[49] G. M. Kopanos, M. C. Georgiadis, E. N. Pistikopoulos, Energy production planning of a network of micro combined heat and power generators, Applied Energy 102 (2013) 1522–1534.